


Obtaining and characterization in tribocorrosive system of nanostructured layers in cobalt matrix with dispersed phase of bioceramic CeO₂ particles
Domain: MATERIALS ENGINEERING

 <p>UNIVERSITAS GALATIENSIS</p>	<p>„Dunarea de Jos University” of Galati www.ugal.ro</p>
 <p>ȘCOALA DOCTORALĂ DE ȘTIINȚE FUNDAMENTALE ȘI INGINEREȘTI PhD</p>	<p>Doctoral School of Fundamental and Engineering Science s http://www.ugal.ro/studii/doctorat/scoli-doctorale/scoala-doctorala-de-stiinte-fundamentale-si-ingineresti</p>
 <p>Competences Center: Interfaces-Tribocorrosion and Electrochemical Systems (CC-ITES) www.cc-ites.ugal.ro</p>	

PHD THESIS

Summary

OBTAINING AND CHARACTERIZATION IN TRIBOCORROSIVE SYSTEM OF NANOSTRUCTURED LAYERS IN COBALT MATRIX WITH DISPERSED PHASE OF BIO-CERAMIC CeO₂ PARTICLES

PhD student,
Eng. Nicoleta - Lucica SIMIONESCU

PhD Supervisor,
Prof. univ. dr. chem. Lidia BENEĂ

Seria I 5: Materials Engineering Nr. 18

GALATI
2020

Obtaining and characterization in tribocorrosive system of nanostructured layers in cobalt matrix with dispersed phase of bioceramic CeO₂ particles
Domain: MATERIALS ENGINEERING

PHD THESIS

Summary

OBTAINING AND CHARACTERIZATION IN TRIBOCORROSIVE SYSTEM OF NANOSTRUCTURED LAYERS IN COBALT MATRIX WITH DISPERSED PHASE OF BIO CERAMIC CeO₂ PARTICLES

PhD Student,
Eng. Nicoleta - Lucica SIMIONESCU

PhD Supervisor,
Prof. univ. dr. chem. Lidia BENEĂ

President

Prof. univ. dr. eng. Elena SCUTELNICU
„Dunarea de Jos” University of Galati

PhD Supervisor,

Prof. univ. dr. chem. Lidia BENEĂ
„Dunarea de Jos” University of Galati

Scientific Board

Prof. dr. habil. eng. Florin MICULESCU
Politehnica University of Bucuresti
Prof. dr. eng. phys. Ionel CHICINAȘ
Technical University of Cluj - Napoca
Prof. dr. habil. Geta CĂRĂC
„Dunarea de Jos” University of Galati

**Seria I 5: Materials Engineering Nr. 18
GALATI
2020**

Seriile tezelor de doctorat sustinute public în UDJG începând cu 1 octombrie 2013 sunt:

Domeniul fundamental ȘTIINȚE INGINEREȘTI

- Seria I 1: **Biotehnologii**
Seria I 2: **Calculatoare și tehnologia informației**
Seria I 3: **Inginerie electrică**
Seria I 4: **Inginerie industrială**
Seria I 5: **Ingineria materialelor**
Seria I 6: **Inginerie mecanică**
Seria I 7: **Ingineria produselor alimentare**
Seria I 8: **Ingineria sistemelor**
Seria I 9: **Inginerie și management în agricultură și dezvoltare rurală**

Domeniul fundamental ȘTIINȚE SOCIALE

- Seria E 1: **Economie**
Seria E 2: **Management**
Seria SSEF: **Știința sportului și educației fizice**

Domeniul fundamental ȘTIINȚE UMANISTE ȘI ARTE

- Seria U 1: **Filologie- Engleză**
Seria U 2: **Filologie- Română**
Seria U 3: **Istorie**
Seria U 4: **Filologie - Franceză**

Domeniul fundamental MATEMATICĂ ȘI ȘTIINȚE ALE NATURII

- Seria C: **Chimie**

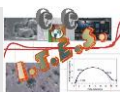
Domeniul fundamental ȘTIINȚE BIOLOGICE ȘI BIOMEDICALE

- Seria M: **: Medicină**

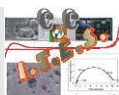
“You don't write because you want to say something; you write because you've got something to say”.

F. Scott Fitzgerald

*** No part of this work may be reproduced or copied without the written consent of the author and the PhD Supervisor.**



Obtaining and characterization in tribocorrosive system of nanostructured layers in cobalt matrix with dispersed phase of bioceramic CeO₂ particles
Domain: MATERIALS ENGINEERING



CC-ITES

Competences Center for Interfaces – Tribocorrosion and Electrochemical Systems

www.cc-ites.ugal.ro

CONTENT

CHAPTER TITLE	Pag.
Thesis title	i
Scientific Board	iii
Motto	v
Content	1
INTRODUCTION	5
CHAPTER I	
SYNTHETIC ANALYSIS OF THE ACHIEVEMENTS IN THE FIELD OF THE DOCTORAL SUBJECT	
	9
1.1. General aspects regarding biomaterials	9
1.2. Different methods and techniques for improving the surfaces of biomaterials	9
1.3. Electrodeposition	10
1.4. Factors influencing the obtaining of functional layers on biomaterials	10
1.5. Dispersed phases used to obtain hybrid and nanocomposite layers	10
1.6. Specific characterization of functional layers on biomaterials in corrosive physiological systems	10
1.7. Specific characterization of functional layers on biomaterials in tribocorrosive systems (corrosion and wear)	11
1.8. Domains of use of functional layers	12
1.9. Partial conclusions	12
1.10. Research directions. The main proposed objectives	12
1.11. Experimental research program	13
CHAPTER II	
RESEARCH METHODOLOGY FOR THE SYNTHESIS OF FUNCTIONAL LAYERS AND THEIR CHARACTERIZATION	
	14
2.1. Materials	14
2.1.1. The support used for electrochemical co-deposition: 304L stainless steel	14
2.1.2. Cobalt matrix for electrodeposition	14
2.1.3. Dispersed phase of cerium oxide (CeO ₂)	14
2.1.4. Solutions and electrolytes used	14
2.2. Methods and techniques for modifying the surfaces of biomaterials	15
2.2.1. Electrochemical cells and electrodes used	15



2.2.2. Experimental working protocols	15
2.3. Techniques for characterizing biomaterials and functional layers	17
2.3.1. Thickness of functional layers	17
2.3.1.1. The layers thickness by cross-sectional scanning electron microscopy.....	17
2.4. Morphological and compositional characterization of biomaterial surfaces and functional layers by scanning electron microscopy (SEM-EDX).....	17
2.5. Microtopographic analysis of biomaterial surfaces and functional layers.....	17
2.6. Structural analysis with the X-ray diffractometer	17
2.7. Microhardness analysis	18
2.8. Hydrophobicity analysis by measuring the contact angle	18
2.9. Evaluation of the tribocorrosive behavior of biomaterials and functional layers in specific biological solutions. Experimental protocol	18
2.10. Partial conclusions	19

CHAPTER III**KINETICS AND MECHANISM OF OBTAINING FUNCTIONAL LAYERS BY ELECTRODEPOSITION**

20

3.1. Mechanism and kinetics of electrodeposition of nanometric dispersed phases with metal matrix	20
3.2. Plotting cyclic voltammetry (CV) curves with and without dispersed phase	20
3.3. Plotting electrochemical impedance spectroscopy (EIS) diagrams for cathodic potentials, with and without dispersed phase	21
3.4. Quantity and current density as a function of time (Q and i) with and without dispersed phase	21
3.5. Partial conclusions	22

CHAPTER IV**THE INFLUENCE OF THE ELECTROCHEMICAL PARAMETERS FOR OBTAINING THE FUNCTIONAL LAYERS ON THEIR PROPERTIES**

23

4.1. The influence of electrodeposition time	23
4.1.1. The influence of the functional layers thickness on the electrodeposition time	23
4.1.2. The influence of electrodeposition time on current efficiency (η [%])	24
4.1.3. The inclusion degree of CeO ₂ nanoparticles as a function of the electrodeposition time	24
4.2. Influence of current density applied to the process	25
4.2.1. Influence of current density on the thickness of functional layers	25



4.2.2. Influence of current density on current efficiency (η [%])	26
4.2.3. Influence of current density on the inclusion degree of CeO ₂ nanoparticles in the cobalt matrix	26
4.3. Partial conclusions	26

CHAPTER V**MORPHOLOGICAL, STRUCTURAL AND TOPOGRAPHIC**

CHARACTERIZATION	27
-------------------------------	-----------

5.1. Morphological and compositional analysis of the biomaterials' surfaces and electrodeposited layers by electron microscopy (SEM-EDX)	27
5.2. Roughness analysis.....	29
5.3. Structural characterization by X-ray diffraction (XRD)	29
5.4. Microhardness analysis of layers	29
5.5. Hydrophobicity characterization of surfaces	29
5.6. Partial conclusions	30

CHAPTER VI**STUDY OF TRIBOCORROSION RESISTANCE (CORROSION AND WEAR) OF OBTAINED BIOMATERIALS AND FUNCTIONAL LAYERS.....**

6.1. Tribocorrosion of the 304L stainless steel	31
6.1.1. Evaluation of electrochemical parameters	31
6.1.1.1. Open circuit potential (OCP)	31
6.1.1.2. Electrochemical impedance spectroscopy (EIS)	32
6.1.2. Evaluation of mechanical parameters, friction coefficient	32
6.1.3. 2D and 3D profile of the wear trace. Wear volume loss in the trace	33
6.1.4. SEM morphological analysis of the wear trace	33
6.2. Co/nano-CeO₂ functional layers	33
6.2.1. Evaluation of electrochemical parameters	33
6.2.1.1. Open circuit potential (OCP)	33
6.2.1.2. Electrochemical impedance spectroscopy at the open potential (EIS)	34
6.2.2. Evaluation of mechanical parameters, friction coefficient	35
6.2.3. 2D and 3D profile of the wear trace. Wear volume loss in the trace depending on the applied normal force	35
6.2.4. Comparative analysis of the wear traces of nanocomposite layers and the 304L stainless steel	36
6.2.5. SEM morphological analysis of the wear trace	36
6.3. Partial conclusions	37

CHAPTER VII

GENERAL CONCLUSIONS, FUTURE PERSPECTIVES	38
---	-----------

7.1. General conclusions	38
---------------------------------------	-----------



7.2. Future perspectives.....	40
--------------------------------------	-----------

CHAPTER VIII

OWN CONTRIBUTIONS AND IMPACT OF THE RESEARCH RESULTS .	41
---	-----------

8.1. Personal contributions	41
8.2. Scientific achievements in the field of the research subject	41
8.2.1. Publications in ISI journals	41
8.2.2. Publication in ISI Proceeding volume	42
8.2.3. Publications in journals indexed in international databases	42
8.2.4. Papers and posters presented at international congresses, workshops and seminars	43
8.2.5. Papers and posters presented at national congresses	45
8.2.6 Research results awards from the Executive Unit for Financing Higher Education, Research, Development and Innovations	47
8.2.7 ISI quotations (Clarivate Analytics)	47
REFERENCES	49

Keywords:

Electrodeposition, tribocorrosion, CeO₂ nanoparticles, cobalt matrix, 304L stainless steel, nanostructuration.

--/--



INTRODUCTION

This study is the result of the research studies carried out within the Competences Center for Interfaces – Tribocorrosion and Electrochemical Systems (CC-ITES), Faculty of Engineering, “Dunarea de Jos” University of Galati, whose director is Professor Lidia BENEĂ, PhD, in collaboration with Laboratoire de Génie des Procédés et Matériaux (LGPM), CentraleSupélec - Université Paris-Saclay, France, coordinated by Professor Pierre Ponthiaux.

The general objective of the research presented in the study is to improve the surface of the 304L stainless steel by the electrochemical co-deposition method in the cobalt metal matrix of dispersed phase of CeO₂ nanoparticles. The electrodeposition method is part of the general methods of obtaining nanomaterials as a **bottom-up** nanotechnology method. Three different concentrations of nanoparticles in the cobalt electrolyte were used, i.e. 10 g/L, 20 g/L, 30 g/L of CeO₂ nanoparticles in order to optimize the stiffening effect of the nano-CeO₂ on improving the tribocorrosive performance of the nanocomposite layers resulted in biological fluids. In particular, this study focused on evaluating the possibilities of these nanocomposite layers (materials) for use in biomedical applications. Furthermore, the study intended to obtain a more thoughtful understanding of the tribocorrosive behavior (corrosion and wear) of the 304L stainless steel support and of the nanocomposite layers obtained in the biological environment which stimulates fluids in the human body.

The specific objectives of the doctoral research project were:

The study of kinetics and the mechanism of obtaining functional layers by electrodeposition of CeO₂ nanometric dispersed phases in the cobalt matrix.

The influence of electrochemical parameters for obtaining nanocomposite functional layers on their properties (the influence of current density and of time applied to the process).

Evaluating the properties of Co/nano-CeO₂ nanocomposite layers from a morphological, structural, topographical (SEM-EDX, XRD, roughness), mechanical (microhardness, wear) point of view, and evaluating the wetting properties of the obtained nanocomposite layers.

Evaluating of the nanostructuring effect of CeO₂ nanoparticles on the cobalt matrix by co-depositing them in the cobalt electroreduction process.

The study of resistance to tribocorrosion (corrosion and wear) of the 304L stainless steel biomaterial and of the nanocomposites' layers obtained by evaluating in-situ electrochemical parameters, evaluating mechanical parameters, in-situ friction coefficient, and by ex-situ methods for characterizing traces of wear.

Collecting data from the data acquisition software and interpreting them.

The doctoral thesis has a number of 192 pages and it has two parts: a theoretical part which represents approximately 12,50 % of the study, and an experimental part that represents personal contributions in the approached field.



The study contains a bibliographic study with a total of 302 references, from which 187 references are from the last 10 years. From the 302 bibliographic references which are presented in the thesis, 2 are personal studies, one of them being ISI listed (Clarivate Analytics).

The study has 87 figures and 20 tables.

The theoretical part of the study (**Chapter I**), **SYNTHETIC ANALYSIS OF THE ACHIEVEMENTS IN THE FIELD OF THE DOCTORAL SUBJECT**, summarizes an overview of the field of biomaterials and its evolution throughout history. First of all, various methods and techniques for improving the biomaterials' surfaces are reviewed. Moreover, factors that influence obtaining some nanocomposite layers on biomaterials are summarized.

It is clear from the specialized literature that the most important parameters that influence obtaining the nanocomposite layers are: the current, particle concentration, the nanoparticles' size, the electrolyte's composition, the electrolyte's pH, the deposition time, and the agitation speed. The dispersed phases used to obtain nanocomposite layers in cobalt matrix are presented.

And at last, the main aspects of corrosion, tribocorrosion of metals and nanocomposite layers in biological environments, as well as the fields of use for biomaterials and nanocomposite layers are presented.

The second part of the study presents the amount of the personal experimental results which are covered in seven chapters.

Chapter II, entitled **RESEARCH METHODOLOGY FOR THE SYNTHESIS OF FUNCTIONAL LAYERS AND THEIR CHARACTERIZATION**, presents the experimental materials, methods and techniques, structured on the two main research directions of the thesis: (1) the study of kinetics and the mechanism of obtaining nanocomposite layers by electrodeposition in the presence and absence of nanometric dispersed phases, and (2) evaluating the properties and the study of the tribocorrosive behavior of nanocomposite layers obtained in the Hank biological solution.

Both obtaining and characterizing the nanocomposite layers required a rigorous substantiation of the electrochemical and mechanical characterization methods that are applied in the field of materials science and engineering. In-situ methods were applied for obtaining, as well as for characterizing the nanocomposite layers properties.

Likewise, the studies were completed with ex-situ methods for evaluating the roughness, microhardness, hydrophobicity, morphology, composition and structure of nanocomposite layers.

In **chapter III**, entitled **KINETICS AND MECHANISM OF OBTAINING FUNCTIONAL LAYERS BY ELECTRODEPOSITION**, the study of kinetics and the nanometric dispersed phase electrodeposition mechanism of cerium oxide in the cobalt matrix by curve-plotting the cyclic voltammetry, electrochemical impedance spectroscopy at different cathodic potentials, and amperometric curves for recording the current, and the amount of electricity as a function of time at different cathodic potentials according to the established experimental protocol, is presented. The study's results have pointed out important information on the mechanism and kinetics of electrodeposition of CeO₂ nanoparticles with cobalt for obtaining Co/nano-CeO₂ nanocomposite layers. The chapter ends with partial conclusions of the study.

Chapter IV, entitled **THE INFLUENCE OF THE ELECTROCHEMICAL PARAMETERS FOR OBTAINING THE FUNCTIONAL LAYERS ON THEIR PROPERTIES** discusses the electrodeposition parameters influence on the nanocomposite layers properties obtained



by electrochemical process. Thereby, it is discussed about the influence of the current density, the electrodeposition time, as well as the nanoparticles concentration from the electrolyte solution on the quality of the nanocomposite layers in terms of the layer's thickness, performance (current efficiency), as well as the degree of inclusion of cerium oxide nanoparticles in the cobalt matrix.

The chapter ends with partial conclusions.

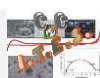
Chapter V, entitled **MORPHOLOGICAL, STRUCTURAL AND TOPOGRAPHIC CHARACTERIZATION**, examines the properties of the nanocomposite materials obtained through classical and advanced characterization methods to highlight the changes made in the surface's morphology and in the structure of the obtained layers. The emphasis is on the characterization of the surfaces obtained with the help of scanning electron microscopy (SEM-EDX) from a morphological and compositional, topographical (roughness), mechanical (microhardness), structural (XRD), biological (hydrophobicity analysis by measuring the contact angle) point of view. The chapter ends with partial conclusions of the study.

Chapter VI, entitled **STUDY OF TRIBOCORROSION RESISTANCE (CORROSION AND WEAR) OF OBTAINED BIOMATERIALS AND FUNCTIONAL LAYERS**, describes the behavior to tribocorrosion (corrosion and wear) of obtained electrodeposited layers as well as the support material used (304L stainless steel). In-situ methods were applied as (open circuit potential, electrochemical impedance spectroscopy, evolution of the friction coefficient depending on the nanoparticles' concentration added in the cobalt electrolyte). Different frictional forces and a constant number of cycles for each studied system were used. Then, ex-situ methods of morphological and topographical characterization for evaluating the depth, width and material loss in the wear traces in comparison on the nanocomposite systems obtained, were applied. At the end of the chapter, partial conclusions are presented about the results of the tribocorrosion resistance of the obtained nanocomposite layers.

Chapter VII, entitled **GENERAL CONCLUSIONS, FUTURE PERSPECTIVES**, summarizes the conclusions on the experimental results of the doctoral thesis, in the field of obtaining and characterizing the tribocorrosion resistance of the obtained nanocomposite structures. Likewise, perspectives and new research directions on the research subject addressed are presented.

Chapter VIII, entitled **OWN CONTRIBUTIONS AND IMPACT OF THE RESEARCH RESULTS**, presents the scientific achievements published in ISI journals (Clarivate Analytics) and in volumes of ISI conferences, publications in journals indexed in international databases and by participating at international and national scientific events.

-- // --





CHAPTER I

SYNTHETIC ANALYSIS OF THE ACHIEVEMENTS IN THE FIELD OF THE DOCTORAL SUBJECT

1.1. General aspects regarding biomaterials

The loss of an organ or part of an organ generates, besides the loss of function, social, as well as psychological disorders. With the evolution of modern medicine, human life expectancy has increased even more due to the use of biomaterials which can solve problems related to the reconstruction of tissues, organs, as well as trauma caused by the passing of the years for the elderly [1].

The term “biomaterial” can be encountered in materials sciences, as well as in clinical medicine and it can be defined as a synthetic material used to replace a part of a living system or in order to function in close connection with the living tissue. A biomaterial is different from a biological material, like the bone, which is a product of a biologic system.

Biomaterials represent an interdisciplinary research area which requires sufficient knowledge from three different fields:

- (1) materials science and engineering processing structure, inter-relationship properties of synthetic and biological materials, including metals, ceramics, polymers, composites, tissues;
- (2) biology, cell physiology, molecular biology, anatomy, animal and human physiology;
- (3) dental clinical sciences, ophthalmology, orthopedics, plastic and reconstructive surgery, cardiovascular surgery, neurosurgery, immunology, histopathology, experimental surgery, veterinary medicine and surgery [4-7].

Generally, the materials used as biomaterials are divided into four categories: metallic, polymer, ceramic and composite [5, 8-11].

1.2. Different methods and techniques for improving the surfaces of biomaterials

Applying coatings is one of the available approaches for improving the materials' surfaces. Over the years, various coating techniques and materials have been used with the purpose of improving the properties of the biomaterials' surfaces.

However, some problems with the coatings have appeared, mainly with delamination or wear of the coating [26-28]. But, researchers' investigations continue to find appropriate materials and techniques to improve the properties of metallic biomaterials. Modifying the biomaterials' surfaces can lead to a more profitable performance in a much shorter time compared to the laborious processes of inventing new possible materials. From an economic point of view, modifying the surface is considered a cheap process because just the surface layer must be modified.

In other words, by modifying the surface, the key physical processes of a biomaterial can be kept while only the exterior surface is modified, in order to adapt to the biointeractions.

The main purpose of the surface modification is to improve the resistance to corrosion, resistance to wear, antibacterial properties, bioadhesion and biocompatibility, while other important requirements, like adequate mechanical resistance and processability, are regulated by the properties of the material. The methods of surface modification can be divided into two big categories: physical and chemical methods.

In most cases, physical methods do not modify the chemical composition of the surface. These



methods can modify the surface's roughness, dimensions and grain limits as well as bevelling. Physical methods often refer to use lasers, plasmas, temperature, polishing and grinding to modify the surface of a material.

Chemical methods are often classified as such because these methods introduce a change in the chemical composition of the surface of a material. The surface can have different chemical properties than the base material.

1.3. Electrodeposition

On the sublayer's surface, some metallic or nonmetallic particles of various dimensions are deposited through an electrolysis process, by chemical modifications that are induced by the passing of a current to improve the material's properties [51,52]. The main advantages of this technique are the low cost, high purity, industrial applicability, etc [53].

Taking into consideration those previously mentioned, we can state that the electrodeposition method over time has led to the development of some nanocomposite coatings with thin film on metallic implants to be used in biomedical applications.

1.4. Factors influencing the obtaining of functional layers on biomaterials

Electrodeposition of nanocomposite coatings with metal matrix is very complex and requires optimizing the process functioning parameters to produce high quality coatings, with improved functional properties. The specialized literature has reported more parameters which are very important in manufacturing composites [67-69]:

Current, concentration of particles, particles' dimension, composition of electrolyte, pH, temperature, deposition time and agitation speed.

1.5. Dispersed phases used to obtain hybrid and nanocomposite layers

Over the years, researchers have made continuous efforts for exploring alternatives to conventional materials making progress regarding the materials' performance, making especially tempting the development area of nanocomposite systems [76]. Nanocomposites are composites in which one or more phases have nanometric dimensions. It is necessary to mention that materials are considered nano when one of the components' dimensions is at nanometric scale, with typical dimensions smaller than 100 nm. Nanocomposite materials are usually known as materials comprised of two or more different materials with well defined interfaces. Generally, a material forms a continuous matrix while the other ensures strengthening [77]. Research regarding nanocomposite coatings by electrochemical co-deposition of fine particles in the metal matrix of electrolytic solutions, has been reported by numerous authors [62, 63, 66, 70, 78-79]. It was discovered that introducing ceramic nanoparticles in the metallic matrix leads to an improvement of the physical and mechanical properties, like resistance to corrosion and wear [80]. Despite the various information which we find in the specialized literature with nanocomposite layers obtained in nickel matrix, there are few with cobalt matrix [81].

It should be noted that the amount of nanoparticles incorporated represents a key parameter for the success of nanocomposite applications with metallic matrix because the quantity of nanoparticles present in the deposited layer largely determines the properties of the nanocomposite, namely resistance to wear, oxidation and higher corrosion [81].

1.6. Specific characterization of functional layers on biomaterials in corrosive physiological systems



Corrosion is defined as deterioration of a material due to the reaction with the environment. The material's degradation can be caused by chemical, electrochemical or physical reactions or by a combination of those [88].

Metals implanted in the organism are exposed to biological liquids which are aqueous liquids that contain different nutrients, organic species, electrolytes, etc [89].

The aqueous nature of body fluids makes the electrochemical processes to be dominant in the corrosion of metallic biomaterials. Different species carried by physiological fluids can affect the mobility of ions inside the fluid, affecting the corrosion speed of metallic implants.

Furthermore, even though body fluids are generally buffer solutions with a pH of approximately 7.4, their pH may modify in case of infections or after surgery [90-92] this significantly influencing the corrosion of materials when they come in contact with them. Taking into consideration that one of the requirements of using a biomaterial is to be resistant to corrosion, modifying the biomaterials' surfaces is one of the few options presently available to reduce corrosion of metallic materials [94].

Lidia B and her team [66] have demonstrated that by increasing the ZrO₂ microparticle content in the Co matrix on a 304L stainless steel sublayer, the resistance to corrosion increases, as well as the microhardness of the layers in comparison to the pure cobalt in Hank's biological corrosion test solution.

1.7. Specific characterization of functional layers on biomaterials in tribocorrosive systems (corrosion and wear)

Tribocorrosion is a degradation process of the material due to the combined effect of corrosion and wear [102]. It is defined [103] as the influence study of chemical, electrochemical and / or biological substances, environmental factors, upon the frictional and wear behavior of the materials' surfaces in mechanical contact with each other and undergoing a relative movement with each other.

Biomaterials used for artificial hip and knee implants are subjected to the static load of the body weight and dynamic loads due to activities such as walking or going up the stairs, and the relative movement between surfaces, due to the range of movement of surfaces. The combined effect of wearing and corrosion can take place on articulated surfaces, but also on other surfaces in contact due to variable loading and unloading, as shown in figure 1.9 (a).

Fracture fixation devices and dental implants (figure 1.9 (b) and 1.9 (c)) are other examples in which the combined effect of wearing and corrosion may take place, due to the small range movement made during activities, like walking or chewing [94].

The thin coatings / films' role and its performances in combined wearing and corrosion conditions is another field of research in tribocorrosion. It is essential to understand the way in which coatings are done in different tribocorrosion conditions, in order to predict the equipment's lifespan and to explore ways of improving it [114].

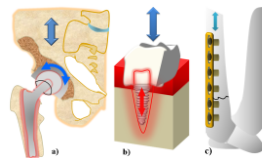


Figure 1.9. Medical devices where tribocorrosion may take place in the human body, like hip implants (a), dental implants (b) and fracture fixation devices (c). The blue arrow represents the typical loading and unloading direction, and the red areas represent the areas that are more liable to corrosion and wear [adapted after 94]

The study of the corrosion and tribocorrosion performance of metallic biomaterials is a necessary field which may help to predict their behavior when they are implanted in the body and to possibly evaluate some new materials with the general purpose of increasing the success of medical implants [94].

1.8. Domains of use of functional layers

Nanocomposites are high performance materials that have rare properties and an annual increase speed, in the 21st century, estimated to 25% [119]. Their perspectives are very important that they are valorous in many fields, starting with packaging to biomedical applications [119]. Throughout many studies done by researchers, it has been shown that using nanocomposites substantially improves mechanical (wear resistance), corrosion resistance, electrical, physical, etc. properties [119]. Nanocomposites devised for different biomedical purposes are often named “biomedical nanocomposites”. The most important biomedical uses of these nanocomposites include drug administration [121], antimicrobial properties [122-123], tissues, bandages [124-125], stem cell therapy, cancer therapy, heart prosthesis, artificial blood vessels, implants and biosensors [126]. Innovative technologies need materials that present unique properties and performances. Processing methods of different types of nanocomposites represent challenges, thus offering opportunities to researchers to surpass problems facing nano-sized materials [119]. They suggest a better performance than the materials with micro dimensions and then they are suitable materials to surpass the restrictions of many materials and devices currently prevalent. Thus, all types of nanocomposites offer opportunities creating a high global interest for these new types of materials [119].

1.9. Partial conclusions

This chapter offers a general overview of the field of biomaterials and of the evolution over the course of history. First of all, various methods and techniques for improving the biomaterials' surfaces are reviewed. Presently, a large number of hospital equipment, medical, dental and laboratory devices were manufactured from various types of metals like steel, due to its adequate mechanical resistance and economic characteristics. Despite their diverse advantages, such materials have some disadvantages like inferior resistance to inferior corrosion /wear, inadequate properties to hardness. To surpass these problems, different improving methods for the biomaterials' surfaces have been suggested, one of them and the most popular being electrodeposition. Then, factors that influence the obtaining of functional layers on biomaterial are summarized and from the specialized literature it turns out that the most important parameters that influence the obtaining of functional layers are: current, concentration of particles, particles' dimension, electrolyte composition, pH, temperature, deposition time and agitation speed. The dispersed phases are presented, used to obtain hybrid layers and nanocomposites in cobalt matrix. And finally, the main aspects of corrosion, tribocorrosion of the metals of functional layers in biological environments, as well as the field of use of the materials of functional layers, are related. In conclusion, the new technologies require materials that present new and / or improved performance of properties compared to the conventional processed components. In this context, nanocomposites are adequate materials to answer the emerging demands arising from scientific and technological advances.

1.10. Research directions. The main proposed objectives

Therefore, the objective of this study is to improve the surface of the 304L stainless steel by the electrochemical method of co-deposition in the cobalt metal matrix in the dispersed phase of CeO₂ nanoparticles. The electrodeposition method falls in the general methods of obtaining nanomaterials as being a bottom-up nanotechnology method. Three different concentrations of nanoparticles in the cobalt electrolyte were used, i.e. 10 g/L, 20 g/L, 30 g/L of CeO₂ nanoparticles in order to optimize the stiffening effect of the nano-CeO₂ on improving the tribocorrosive performance of nanocomposite layers resulted in biological fluids. Moreover, this study aimed to obtain a deeper understanding of the tribocorrosive (corrosion and wear) behavior of the 304L stainless steel support and of the nanocomposite layers obtained in biological environment that stimulates the human body fluids.

For this, a bibliographic study of the most recent national and international research regarding



the nanocomposite hybrid layers has been carried out with possible biomedical applications in tribocorrosive, corrosive, etc. systems.

The objective was to optimize the working parameters in order to obtain nanocomposite hybrid layers.

The study of kinetics and the mechanism of obtaining functional layers by electrodeposition of CeO₂ nanometric dispersed phases in the cobalt matrix.

The influence of electrochemical parameters for obtaining nanocomposite functional layers on their properties (the influence of current density and of time applied to the process).

Evaluating the properties of Co/nano-CeO₂ nanocomposite layers in terms of morphology, structure, topography (SEM-EDX, XRD, roughness), mechanical (microhardness, wear) and evaluating the wetting properties of the obtained nanocomposite layers.

Evaluating the nanostructure effect of CeO₂ nanoparticles on the cobalt matrix by co-depositing them in the cobalt electroreduction process.

The study of resistance to tribocorrosion (corrosion and wear) of the 304L stainless steel biomaterial and of the nanocomposites' layers obtained by evaluating in-situ electrochemical parameters, evaluating mechanical parameters, in-situ friction coefficient and by ex-situ methods for characterizing traces of wear.

Collecting data from the data acquisition software and interpreting them.

1.11. Experimental research program

Within the Competences Center For Interfaces – Tribocorrosion and Electrochemical Systems (CC-ITES) the following activities were carried out:

- Preparing the solutions used in the kinetics of electrodeposition of nanocomposite layers and for the study of tribocorrosion behavior.
- Preparing the 304L stainless steel samples (used as support): cutting, cleaning, isolating, contact, weighing before and after electrodeposition.
- Optimizing the working parameters for kinetics as well as for electrochemical deposition (electrolyte volume in the electrochemical cell, distance between anode and cathode, the pH of the electrolyte solutions used, etc.).
- Obtaining the nanocomposite hybrid functional layers.
- Morphological and compositional characterization of the biomaterials' surfaces and of the functional layers by scanning electron microscopy (SEM-EDX).
- Analysis of the roughness and the contact angle.
- Structural analysis with the X-ray diffractometer.
- Interpreting the obtained results with different simulation programs and correlating them.
- Microhardness of the layers.

Within Laboratoire de Génie des Procédés et Matériaux (LGPM), CentraleSupélec - Université Paris-Saclay, França:

- Due to the collaboration agreement between CC-ITES (“Dunarea de Jos” University of Galati) <https://www.centralesupelec.fr/fr/laboratoire-genie-des-procedes-et-materiaux-lgpm-ea-4038> in-situ tribocorrosion experiments were carried out on a tribocorrosion meter (an adapted tribometer comprised of a Solartron 1287 electrochemical potentiostat associated with a Solartron 1255, guided with the help of a computer using CorrWare and Zware softwares). This device can acquire electrochemical results from imposed mechanical parameters (speed, normal pressing force) as well as mechanical data (coefficient of friction) depending on the same default mechanical parameters. Also, ex-situ characterization tests.

Regarding the processing, modeling and interpreting of the experimental data, these were carried out within the research center (CC-ITES) by the doctoral student.



CHAPTER II

RESEARCH METHODOLOGY FOR THE SYNTHESIS OF FUNCTIONAL LAYERS AND THEIR CHARACTERIZATION

In this chapter the main used experimental materials, techniques and methods are described for carrying out the experimental research of the doctoral thesis entitled *Obtaining and characterization in tribocorrosive system of nanostructured layers in cobalt matrix with dispersed phase of bioceramic CeO₂ particles*. Hence, the support layer on which the deposits were done is described, the metallic matrix used, description of the type of nanoparticles used, description of the working protocols and of the used electrolytes, schematic representation of all equipment and electrochemical cells used for completing this work.

2.1. Materials

2.1.1. The support used for electrochemical co-deposition: 304L stainless steel

In this study 304L stainless steel was used as a support layer for electrodeposition, purchased from Direct Line Inox, Bucharest, in the form of sheets with a thickness of 1.2 mm.

2.1.2. Cobalt matrix for electrodeposition

The cobalt matrix for electrodeposition was purchased from the Godfellow company, in the form of sheets with the dimensions of 50 mm x 50 mm, 2 mm thickness, 99.9% purity.

2.1.3. Dispersed phase of cerium oxide (CeO₂)

For obtaining nanocomposite hybrid layers in cobalt matrix, CeO₂ nanoparticles in the form of nanopowder (CAS no. 1306-38-3) were used as dispersed phase purchased from the Sigma Aldrich company with average particle size of < 25 nm, packed in vials weighing 25 g.

2.1.4. Solutions and electrolytes used

The following electrolytes were used for the experimental part of electrodeposition and characterization at tribocorrosion:

1. Cobalt electrolyte used for the electrodeposition process, as well as for studying the mechanism and kinetics of electrodeposition of nanometric dispersed phases with metallic matrix.
2. The solution which simulates the biological fluid known as Hank, used for the tribocorrosive tests.

All the electrolytes used for the experimental part have been freshly prepared with chemical reagents of analytical purity purchased from the Merck company, with distilled, purified water kept in 5L sterile vials in order to have sufficient quantity, as well as for having constant parameters during the entire electrochemical process.



2.2. Methods and techniques for modifying the surfaces of biomaterials

2.2.1. Electrochemical cells and electrodes used

For carrying out this research, 3 electrochemical cells were used (1 – cell for studying kinetics, 2 – cell for electrodeposition, 3 – cell for tribocorrosive tests). For the study of the mechanism and kinetics of electrodeposition of nanometric dispersed phases with metallic matrix, as well as for realizing the electrodeposition process, a VoltaLab PGZ 301 potentiostat / galvanostat connected to a laptop on whose software functions the Voltmaster4 program (a device available in the CC-ITES research center) was used.

The electrochemical cells were made with the lather so that the position of the electrodes is vertical and parallel, as well as for keeping a constant distance between the electrodes during the entire process.

Like in the case of the electrochemical cell used in studying the mechanism and kinetics of the nanometric dispersed phases in cobalt matrix, the same device was used with the same functioning principle, only that the configuration of the working electrode was changed (for electrochemical depositions 304L stainless steel sheets were used as support layer) as well as the configuration of the anode (respectively, a cobalt sheet was used for these processes), the reference electrode remaining the same.

The corrosion and wear (tribocorrosion) tests were done using a unidirectional tribometer (pin on disk). The tribometer is modified for working with an electrochemical cell formed of three electrodes. Therefore, the samples used as working electrode (WE), i.e. nanocomposite hybrid layers obtained by the electrodeposition process are mounted in horizontal position in the electrochemical cell, this being connected to a potentiostat.

For the tribocorrosive tests, a Solartron Instruments 1287 potentiostat / galvanostat was used with a SI 1255 frequency response analyzer guided with the help of a computer using CorrWare and Zware softwares, used to monitor electrochemical parameters during the friction tests in corrosive environment. Subsequent data analysis was performed by CView and Zview softwares from Scribner Associates, Inc. The platinum wire is used as a counter electrode (CE) and as reference electrode (RE) is used Ag / AgCl (KCl, E = + 199 mV vs. NHE at 22°C saturated solution). These electrodes are positioned in the tribocorrosive cell in a way that only 3 cm² of the working electrode's surface is exposed to the electrolyte.

During the tribocorrosion test, the normal force, peripheral force, friction coefficient, number of cycles, as well as the electrochemical parameters (open circuit potential, electrochemical impedance spectroscopy) were permanently monitored.

2.2.2. Experimental working protocols

a) The experimental protocol used to study the kinetics electrodeposition:

Type of equipment used:

PGZ 301 Potentiostat / Galvanostat guided by laptop with the help of the VoltaMaster4 software.

Preparing the working electrode (WE):

As working electrode (cathode) a brass cylinder was used, the samples were cut, tapped at the lathe and the surface was isolated with epoxy resin for a well-delimited active surface of 2,21 cm². For the electric contact, a metal rod of brass tapped at the lathe, screwed at the top of the cathode cylinder was used. Each sample, before it was submerged in electrolyte, was cleaned with antitarnish paper, degreased and pickled, after which it was rinsed with distilled water and dried in the oven, and after each measurement, the cobalt anode was cleaned with 1:1 hydrochloric acid for 2 minutes.

Preparing the counter electrode (CE):

- As anode, a circular electrode of pure Co was used (which is the metallic matrix in the electrodeposited layer) with electrical contact whose diameter was $\varnothing = 7$ cm.
- The pure Co anode, before it was submerged in the solution, it was degreased with alcohol, rinsed with distilled water, dried in the oven.

Reference electrode (RE):

- Ag/AgCl (with KCl saturated solution) , E = + 199 mV vs. NHE at 22°C.

Electrolysis cell:

- is composed of three electrodes (WE (cathode), CE (anode), RE);
- volume of 160 mL of electrolyte;
- with electromagnetic agitation system;
- special cap made at the lathe, so that the position of the electrodes is easily done at the same distance for each measurement;

Working parameters:

- pH = 4.21; temperature = 22 ± 1 °C; magnetic agitation = 300 rpm.

Electrochemical measurements:

- Plotting the cyclic voltammetry (CV) curves with and without dispersed phase;
- Plotting electrochemical impedance spectroscopy (EIS) diagrams to cathodic potentials with and without dispersed phase;
- Current quantity and density depending on time (Q and i) with and without dispersed phase.
- Electrochemical measurements from the deposition kinetics were repeated 4 times in order to see if the results are reproducible.

b) The experimental protocol used to perform the electrodeposition process:

For realizing the nanocomposite hybrid layers the same equipment previously mentioned at point (a) was used.

Preparing the working electrode (WE):

As working electrode (cathode), a 304L stainless steel sheet was used, the samples were marked, cut, dotted, drilled and burred and the electrical contact was made with the help of a copper wire, isolated with epoxy resin to have a well-delimited surface of 4.25 cm². The samples (the 304L stainless steel support layer) were cleaned according to the experimental control. They were mechanically cleaned with antitarnish paper for removing irregularities, chemical degreasing with a NaOH 50 g / L solution by total submersion of the sample in the solution for 10 minutes at a bath temperature of 70° C with the purpose of removing grease from the material's surface, chemical pickling with a 1:1 HCl solution for 5 min, rinsed with distilled water, afterward immediately introduced in the electrolyte bath.

Preparing the counter electrode (CE):

- As anode, a pure Co sheet was used, with electrical contact whose active surface was 9 cm². The pure Co anode, before it was submerged in the solution, was degreased with alcohol, rinsed with distilled water, dried in the oven, and after each measurement the cobalt anode was cleaned with 1:1 hydrochloric acid for 2 minutes.

Reference electrode (RE):

- Ag/AgCl (with KCl saturated solution) , E = + 199 mV vs. NHE at 22°C.

Electrolysis cell:

- Is composed of three electrodes with a 160 mL electrolyte volume. The nanoparticles' dispersion was made with the help of an electromagnetic agitation system and the magnetic agitation was 300 rotations per minute.

Working parameters:

- The electrolyte's pH was maintained at 4.21 adjusted with HCl as needed, measured before, during and after the electrodeposition process finished. The deposits were done at room temperature = 22 ± 1 °C;



Imposed electrochemical measurements:

- Plotting chronopotentiometry curves in the absence of CeO₂ nanoparticles in the current density range 23 mA/cm², 48 mA/cm², 72 mA/cm² with a duration of 30 minutes, 60 minutes and 90 minutes noted in this study as pure Co;
- Plotting chronopotentiometry curves in the presence of CeO₂ nanoparticles (nanoparticles whose amount present in the cobalt electrolyte is 10 g / L marked Co/nano-CeO₂ – 10 g/L , 20 g / L (Co/nano-CeO₂ – 20 g/L) and 30 g /L (Co/nano-CeO₂ – 30 g/L) in the current density range 23 mA/cm², 48 mA/cm², 72 mA/cm² with a duration of 30 minutes, 60 minutes and 90 minutes.

2.3. Techniques for characterizing biomaterials and functional layers

2.3.1. Thickness of functional layers

2.3.1.1. The layers thickness by cross-sectional scanning electron microscopy

For determining the thickness of the pure cobalt and of the obtained Co/nano-CeO₂ nanocomposite layers one of the most popular techniques was used to characterize and that is scanning electron microscopy (SEM) whose detailed description is in subchapter 2.4. To visualize the thickness of the layers, the samples were prepared as follows: they were cut in cross section, cleaned with alcohol, dried in the oven, coated with Gold (Au) with a thin film whose thickness is 5nm, fixed on a metal support with a carbon tape for better electrical conductivity.

2.4. Morphological and compositional characterization of biomaterial surfaces and functional layers by scanning electron microscopy (SEM-EDX)

Within the thesis, SEM analysis were carried out for a number of 9 samples from each study (each sample being gilded with a layer of gold whose thickness was 5 nm) and evaluated for surface and section modifications. FEI QUANTA 200 scanning electron microscope was used to determine and compare the morphological variations between the samples with pure cobalt layers and samples with Co/nano-CeO₂ nanocomposite layers. Also, the samples were analyzed in terms of chemical composition by X-ray dispersive spectroscopy (EDX) with the help of the EDAX Genesis data acquisition software.

2.5. Microtopographic analysis of biomaterial surfaces and functional layers

For testing the roughness of the samples' surfaces, a Surftest SJ-210 portable roughness meter (Mitutoyo, Japan) was used. The analysis length was 4 mm with a scan speed of 0.25 μm / s and 9 measurements were done for each sample, and afterward, the averages of the extracted values will be presented.

2.6. Structural analysis with the X-ray diffractometer

According to the X-ray diffraction test, registered with the help of the Dron 3 device, using a Cobalt anode (Co, $\lambda_{K\alpha} = 1.790300 \text{ \AA}$), with a tension (U) of 30 kV, intensity (I) of 20 mA, with a pace of 0.05° / s, on a range between 15 - 90°, exposure time 3 seconds, and the total / sample time 2 h and 13 minutes, and the obtained specters were correlated using standardized data of the Match! 3 software for identifying phases (<http://www.crystalimpact.com/match>). The results were correlated with the



Crystallography Open Database, COD, identifiable with a 9 number format code. The microstructure and morphology of the deposited material changes and the X-ray diffraction pattern changes accordingly. The differences in concentration or the type of change directly influenced the results by different changes in the X-ray diffraction pattern. The X-ray diffraction measurement is one of the necessary steps in the characterization of these nanocomposite hybrid materials, due to the successful elucidation of crystalline structures in diffraction patterns [212].

2.7. Microhardness analysis

The microhardness was measured with the help of the Leitz microhardness tester (Wetzal GMBH, Wetzlar, Germany), this being equipped with a standard Vickers diamond penetrator (indenter of 0.2 kgf / mm²). On each sample, a set of 5 measurements was done (and the exposure period for each measurement was of 15 seconds).

2.8. Hydrophobicity analysis by measuring the contact angle

For determining the wetting of the obtained nanocomposite layers, in this study an OCA 15 EC equipment, Dataphysics, Germany, was used, connected to a laptop, guided with the help of a software named SCA20, in whose test syringe the Hank biological solution was introduced, the volume of solution measured for each measurement (9 measurements per sample) was 10 μL.

2.9. Evaluation of the tribocorrosive behavior of biomaterials and functional layers in specific biological solutions. Experimental protocol.

To investigate the corrosion and wear behavior (tribocorrosion) of the obtained nanocomposite hybrid layers, a potentiostat called Solartron Instruments 1287 was used, which has a SI 1255 frequency response analyzer.

The used working electrodes (WE) were:

- The layers noted in this study named pure Co, Co/nano-CeO₂ – 10 g/L, Co/nano-CeO₂ – 20 g/L and 30 g/L (Co/nano-CeO₂ – 30 g/L) whose active surface for these tests was 3 cm².

Electrolysis cell:

- Is composed of three electrodes: the working electrode, the reference electrode (with KCl saturated solution), E = + 199 mV vs. NHE, counter electrode (platinum wire), with a volume of 450 mL Hank electrolyte, and the tests were conducted at room temperature and every time the solution was changed.

- The pin used is an alumina cylinder (Al₂O₃) (7 mm in diameter), vertically mounted on a rotating head over the sample. The lower spherical end of the pin (radius = 100 mm) can be applied on the layer's surface with an adjustable normal force which was 1 N, 3 N, 5 N for comparative investigations to tribocorrosion of pure cobalt and nanocomposite layers. When force is applied, the end of the needle draws a circular wear surface (10 mm in diameter) on the sample's active surface.

Electrochemical measurements:

- Measuring the open circuit potential (OCP) of the obtained layers in comparison with the Ag / AgCl reference electrode, from immersion for a period of 18 hours until reaching a stable value without friction.

- Measuring the electrochemical impedance spectroscopy (EIS) to the measured open circuit potential and stabilised in the Hank biological solution without friction.

- Measuring the friction coefficient where the open circuit potential is measured vs. the Ag / AgCl reference electrode.

- Measuring the electrochemical impedance spectroscopy (EIS) to the open circuit potential and stabilised in the Hank biological solution during friction.



- Measuring the surface's open circuit potential (OCP) after the friction tests are stopped for 120 minutes, so as to observe the repassivation capacity of the tested surfaces.
- Measuring the electrochemical impedance spectroscopy (EIS) to the open circuit potential and stabilised in the Hank biological solution after the friction tests were stopped.
- The wear tests were performed by applying three forces: 1N, 3N and 5N at a constant speed of 120 rpm with a period of 5000 cycles.
- The tribocorrosion tests were repeated at least three times to see if there was reproducibility.

2.10. Partial conclusions

This chapter describes in detail the main materials used to realize nanocomposite hybrid layers, i.e. the support layer (304L stainless steel). The dispersed phase of CeO₂ used, the cobalt matrix is described and the solutions and electrolytes used for preparing and obtaining the nanocomposite layers are presented.

The electrochemical cells used, the experimental work protocols and the work equipment used to carry out this study are presented schematically.

The main characterization techniques and instruments of the respective materials, use of the scanning electron microscope for the morphological and compositional characterization, as well as in cross-section of the obtained nanocomposite hybrid layers, are presented.

For the structural characterization with the X-ray diffractometer, the method's principle is presented, the description of the used equipment and the spectra's interpreting program is also presented.

The surface improvement by adding nanometric dispersed phase of cerium oxide to the cobalt matrix by electrodeposition technique has improved the wetting, microhardness, roughness properties, as well as an increase of resistance to corrosion and wear (tribocorrosion) of the obtained nanocomposite layers.

CHAPTER III

KINETICS AND MECHANISM OF OBTAINING FUNCTIONAL LAYERS BY ELECTRODEPOSITION

Electrochemical kinetics is the electrochemistry field that studies the speed of electrochemical processes. This includes studying how the process conditions, like the concentration and electrical potential, influence the rate of oxidation and reduction reactions that occur on the surface of an electrode, as well as an investigation of electrochemical reaction mechanisms. Due to electrochemical phenomena which take place at the interface between an electrode and an electrolyte, there are accompanying phenomena of electrochemical reactions that contribute to the total reaction rate [228].

3.1. Mechanism and kinetics of electrodeposition of nanometric dispersed phases with metal matrix

The electrodeposition mechanism refers to the fact that the moment when nanoparticles are introduced in the solution, a layer of adsorbed ionic species is created on their surface, forming around each nanoparticle and electrically diffuse double layer. Under the influence of the electric current and of the electrolyte's agitation, the nanoparticles are transported on the cathode's surface and when the distributed ionic species on the nanoparticles are reduced, the nanoparticles are integrated into the layer. It should be noted that ionic species can not pass through a charging transfer stage without intermediate, thus the first step in depositing a metal should be its chemical transformation in an electroactive species. This stage takes place during the diffusion transport of ionic species to the electrode surface which takes place inside the electrical double layer [229].

3.2. Plotting cyclic voltammetry (CV) curves with and without dispersed phase

In this study the cyclic voltammetry method was used to determine the potential in which the cobalt's electro-crystallization is done, thus the potential measurement was done in the potential range, which starts from -1200 mV to -278 mV (vs. Ag/AgCl) with a scanning speed of 3 mV / sec.

The cyclic voltammetry curves of Co and Co / nano – CeO₂ nanocomposite systems with different concentration of CeO₂ nanoparticles recorded with a scanning speed of 3 mV / sec, are presented in Figure 3.1.

As shown in figure 3.1., adding CeO₂ nanoparticles in the solution leads to a shift of the cobalt reduction curve to more positive values with increasing the concentration of CeO₂ nanoparticles. The same behavior is reported in the case of the nano-TiO₂ particles from the nickel's electrodeposition from a Watts electrolyte [232]. The shift of the reduction potential can be caused by CeO₂ nanoparticles added in the electrolyte, thus modifying the mechanism of cobalt nucleation during electrodeposition. Taking into consideration a constant value of the cathodic potential of -0.9 V (relative to Ag/AgCl), in figure 3.1. displays that the current density takes the lowest cathodic value for the pure Co system being equal with -34.26 mA / cm² ($t = 98$ sec).

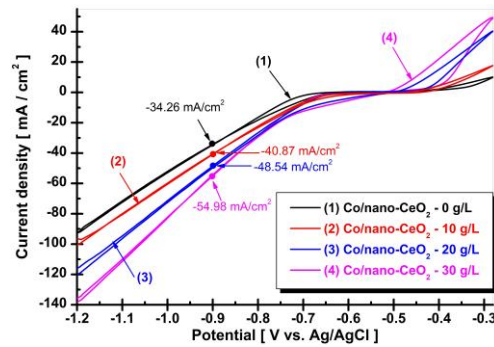


Figure 3.1. Cyclic voltammograms for: (1) pure Co, (2) Co/nano- CeO_2 – 10 g/L, (3) Co/nano- CeO_2 – 20 g/L and (4) Co/nano- CeO_2 – 30 g/L

For the Co/nano- CeO_2 – 10 g/L system, the current density reveals an increased cathodic value of $-40,87 \text{ mA / cm}^2$ ($t = 98 \text{ sec}$), for the Co/nano- CeO_2 – 20 g/L system, the current density shows an additional cathodic value than the Co/nano- CeO_2 – 10 g/L system this value being of $-48,54 \text{ mA / cm}^2$ ($t = 98 \text{ sec}$). And for the Co/nano- CeO_2 – 30 g/L system, the current density reaches the highest cathodic value of $-54,98 \text{ mA / cm}^2$ ($t = 98 \text{ sec}$) than the other systems. These results confirm the process activation of electroreduction of the Co matrix in the presence of CeO_2 nanoparticles, demonstrating that one of the intermediate stages of co-deposition is the metallic ions absorption on the particles' surface and their movement towards the cathode. Similar results regarding the tendency to increase the current density during the adding of nanoparticles to electrodeposition has been noticed by other authors as well [232-233].

3.3. Plotting electrochemical impedance spectroscopy (EIS) diagrams for cathodic potentials, with and without dispersed phase

Electrochemical impedance spectroscopy (EIS) is a non-destructive method which won the interest in the last decades, especially for the electrochemical impedance spectroscopy answers during electrodeposition due to the possibility to determine more parameters of the ex systems for characterizing the electrode's processes and for determining the electrochemical systems' kinetics [234]. One of its advantages is the possibility to investigate the electrode's surface, the adsorbed species and the increase of the layers. The impedance specters of metal / alloy deposition processes usually present one or more loops (capacitive or inductive) [239].

The electrochemical impedance spectroscopy (EIS) measurements were registered in the cobalt electrolyte in the presence and absence of the CeO_2 nanoparticles in order to observe the effect which the nanoparticles have upon the electrodeposition mechanism. These measurements were done at different cathodic potentials between -750 and -840 mV (vs. Ag/AgCl).

3.4 Quantity and current density as a function of time (Q and i) with and without dispersed phase

In this research, the chronoamperometry method is used to determine the electrodeposition method of the cobalt in the presence and absence of the CeO_2 nanoparticles at different cathodic potentials (ranging from -750 mV to -840 mV (vs. Ag/AgCl)) for a deposition time of 300 seconds.

Chronocoulometry is a method that measures the surface's interfacial properties by the amount of electricity consumed in the electrodeposition of metal or composite.

3.5. Partial conclusions

The cobalt's electrodeposition from an electrolyte bath, to which different concentrations of CeO₂ nanoparticles were added, was studied at different cathodic potentials (vs. Ag/AgCl) by the following methods: cyclic voltammetry (CV), electrochemical impedance spectroscopy (EIS), chronoamperometry and chronocoulometry.

The study of cyclic voltammetry shows that by adding CeO₂ nanoparticles in the solution leads to a shift of the cobalt's reduction curve to more positive potential values with the increase of the nanoparticles concentration in electrolyte, thus affecting the nucleation mechanism of the cobalt.

The impedance specters are influenced by adding the CeO₂ nanoparticles and, consequently, the charge transfer resistance decreases for all nanocomposite systems compared to the pure Co system.

By increasing the CeO₂ nanoparticles concentration the cobalt's reduction is active, the ionic transport is improved, as well as the density of the nucleation sites.

From the chronocoulometry curves of the pure Co and of the Co/nano - CeO₂ systems, an increase of current density is highlighted with the increase of the CeO₂ nanoparticles concentration, due to the increase of the active surface.

As a final conclusion, the CeO₂ nanoparticles induce structural modifications of the cobalt matrix by increasing the number of favorable sites for the cobalt's nucleation.

CHAPTER IV

THE INFLUENCE OF THE ELECTROCHEMICAL PARAMETERS FOR OBTAINING THE FUNCTIONAL LAYERS ON THEIR PROPERTIES

In this chapter, we studied the influence of some of the most important electrochemical parameters applied to the electrodeposition process, i.e. time influence as well as current density on the thickness of the obtained functional layers compared to the pure Co layers on the electrodeposition efficiency, as well as on the degree of inclusion of cerium oxide nanoparticles present in the nanocomposite layers obtained in this study. At the same time, this chapter has the purpose to enhance the formal knowledge which a young researcher should have on the way in which time and current density applied to the process influence the electrodeposition of functional layers, precisely to conclude whether the conditions imposed on the process of electrodeposition were optimal. Hence, optimal conditions lead to improving the electrodeposition's quality, reducing the production costs and last but not least for the ultimate goal, that of improving the resistance to corrosion, wear or to tribocorrosion, etc.

4.1. The influence of electrodeposition time

4.1.1. The influence of the functional layers thickness on the electrodeposition time

As I mentioned in subchapter 1.4, time is one of the factors which affects the electrodeposition process. Generally, the thickness of the layers increases in direct proportion to the time and current density according to Faraday's laws, the amount of electricity (Q measured in Coulombi) is directly proportional to the electric current intensity (I measured in Amperes) or time (t measured in seconds) [241].

In order to observe how the thickness of the functional layers fluctuates depending on time in the electrodeposition process, the variation of three times taken as a multiple of 30 minutes, respectively 30 minutes, 60 minutes and 90 minutes, was taken into account, both for pure Co and for nanocomposite functional layers using different concentrations of CeO₂ nanoparticles (10 g/L, 20 g/L, 30 g/L) for the three applied current densities (23 mA/cm², 48 mA/cm², 72 mA/cm²).

From the analysis of the layers' thickness, it can be noticed that with the increase of electrodeposition time and of the dispersed phase concentration (CeO₂ nanoparticles), the thicknesses of the obtained layers also increase.

For pure Co, at the time of 30 minutes, the layer's thickness has a value of 10.63 μm, for Co/nano-CeO₂ – 10 g/L can be noticed that the layer's thickness increases in contrast with the pure Co at a value of 13.52 μm. Once with the increase of the CeO₂ nanoparticles concentration to 20 g/L, the thickness of the layer reaches a value of 19.81 μm at the same deposition time and for Co/nano-CeO₂ – 30 g/L the layer thickness has a value of 23.70 μm. These values of the layer's thickness increase with the time increase for all systems reaching to the time of 90 minutes to 24.11 μm for the pure Co layer, 30.02 μm for Co/nano-CeO₂ – 10 g/L, 36.13 μm for Co/nano-CeO₂ – 20 g/L and 41.35 μm for Co/nano-CeO₂ – 30 g/L.

As the CeO₂ nanoparticles increase in the electrolyte, the thicknesses of the hybrid nanocomposite layers slightly increase in comparison with the pure cobalt layer at the same deposition



time, denoting the incorporation of cerium oxide in the cobalt matrix. The increase of the layers' thickness with the electrodeposition time has been reported in the specialized literature by other authors as well [242-244, 115].

4.1.2. The influence of electrodeposition time on current efficiency (η [%])

In figure 4.3., the time influence (30, 60, 90 min) on the electrodeposition efficiency for Co/nano-CeO₂ nanocomposite layers with different CeO₂ concentrations (10, 20, 30 g/L) is highlighted, compared to the layers without the addition of nanoparticles (pure Co) to different current densities (23, 48, 72 mA/cm²).

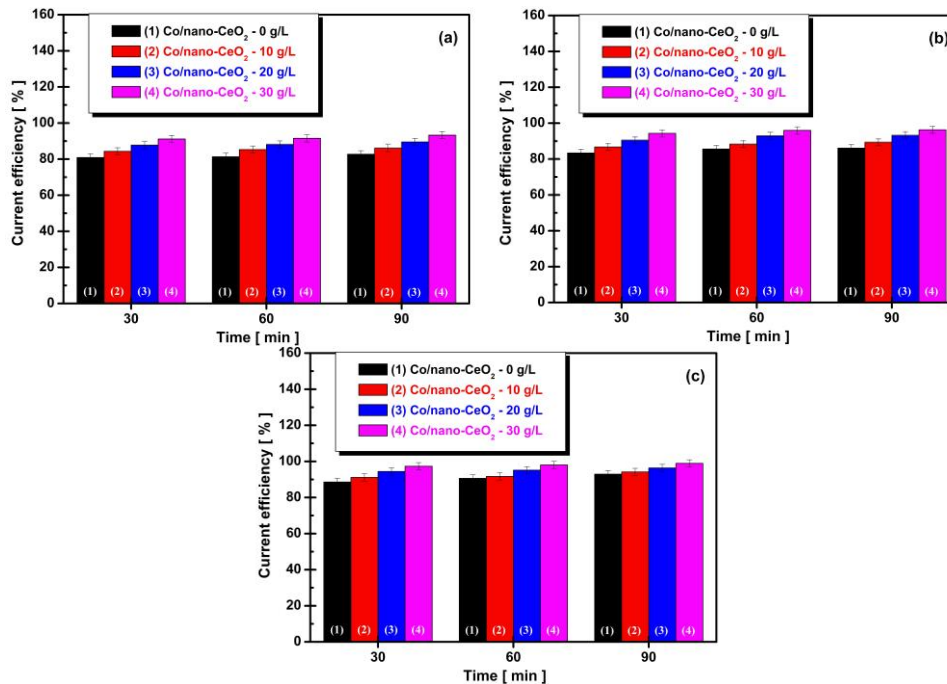


Figure 4.3. Variation of the current efficiency according to the deposition time for: (1) pure Co; (2) Co/nano-CeO₂ – 10 g/L; (3) Co/nano-CeO₂ – 20 g/L and (4) Co/nano-CeO₂ – 30 g/L at current densities of: (a) 23 mA/cm², (b) 48 mA/cm² and (c) 72 mA/cm²

From figure 4.3 (a), it can be observed that for the pure Co layer, at the deposition time of 30 minutes and the current density of 23 mA/cm², the deposition efficiency has the lowest value starting from 80.91 %, this value increasing with the deposition time reaching the time of 90 minutes at an efficiency value of 82.69 %, while the efficiency value for the Co/nano-CeO₂ – 10 g/L layer at the same time (30 min.) increases with a value of 84.33 % reaching the deposition time of 90 minutes to 86.10 %. As the concentration of CeO₂ nanoparticles in the electrodeposition solution increases, the efficiency value increases to a value of 87.65 % for the Co/nano-CeO₂ – 20 g/L layer at the time of 30 minutes, reaching a value of 89.52 % at the time of 90 minutes. In the case of the Co/nano-CeO₂ – 30 g/L layers, at the time of 30 minutes, the efficiency begins at a value of 91.16%, and this value increases with the time deposition and in this case, it reaches at the end of the 90 minutes a value of 93.31%.

This trend of increasing the efficiency of the electrodeposition current with the increase of the deposition time, has been reported in the specialized literature by other authors as well [115, 244-245].

4.1.3. The inclusion degree of CeO₂ nanoparticles as a function of the electrodeposition time

The degree of inclusion of cerium oxide nanoparticles was calculated from the SEM-EDX elemental analysis, depending on the three deposition times (30, 60, 90 minutes) at current densities of 23, 48, 72 mA/cm^2 . The data for the EDX analysis were collected from the entire scanning area of the samples to determine the inclusion percentage of the Ce element in the cobalt matrix.

The inclusion percentage of the CeO_2 nanoparticles in the Co matrix was determined by transforming the Ce mass percentage (wt.%) from the general analysis of the molecular mass of CeO_2 . The standard atomic mass of the Ce element has a value of 140.116 g/mol.

Taking into consideration the exemplified diagrams, we can state that the inclusion degree of the CeO_2 nanoparticles in the cobalt matrix increases at the same time with the time increase for all studied systems (Co/nano- CeO_2 – 10 g/L, Co/nano- CeO_2 – 20 g/L, Co/nano- CeO_2 – 30 g/L) and at the same time with the increase of nanoparticles concentration from the electrodeposition electrolyte.

The same trend of increasing the degree of nanoparticles in different metal matrices with increasing the deposition time and increasing the concentration of nanoparticles in the electrolyte was observed by other authors, as well, in their doctoral theses [115, 244].

4.2. Influence of current density applied to the process

4.2.1. Influence of current density on the thickness of functional layers

The current density plays an important role in controlling the deposition speed which, in turn, will affect the concentration, composition and morphology of the included particles in layers. Moreover, it influences the nanocomposite layers' thickness, so that the current density leads to an increase of the coatings thickness, and a low density of the current will produce films with big surface flaws [77]. In order to observe the influence of the current density on the layer's thickness obtained for this study, in figure 4.5., the diagrams with the values obtained from the thickness of the layers are shown, measured in cross-section at SEM for the three current densities applied to the electrodeposition process: 23 mA/cm^2 , 48 mA/cm^2 , 72 mA/cm^2 for all nanocomposite layers obtained by adding CeO_2 nanoparticles in the electrolyte in a concentration of 10 g/L, 20 g/L and 30 g/L in comparison with the pure Co layers at the three deposition times applied to the process (30', 60', 90').

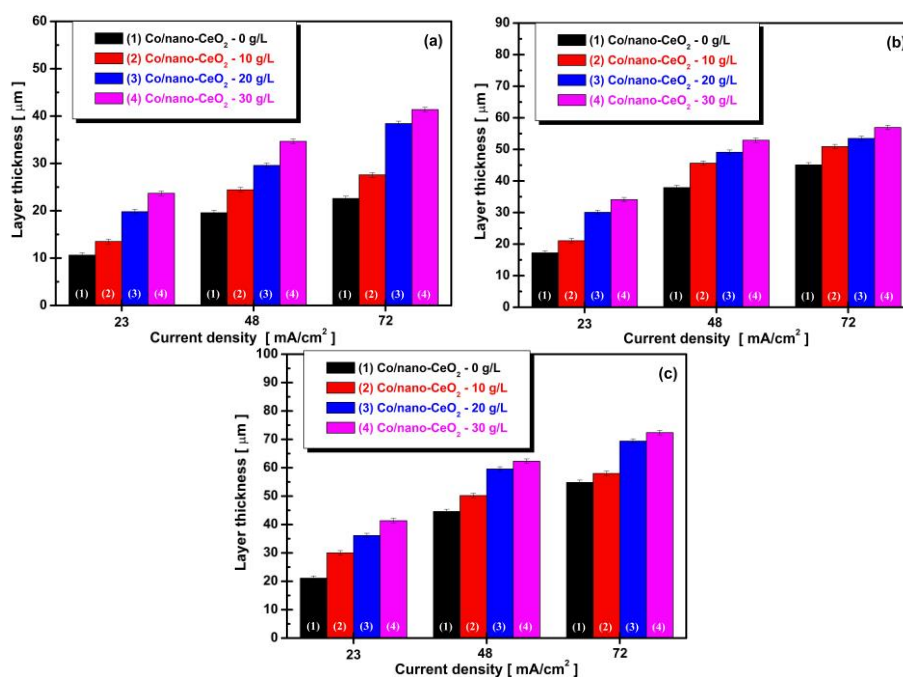


Figure 4.5. Variation of layer thickness according to the current density obtained by scanning electron microscopy in cross section for: (1) pure Co; (2) Co/nano- CeO_2 – 10 g/L; (3) Co/nano- CeO_2 – 20 g/L and (4) Co/nano- CeO_2 – 30 g/L at the three electrodeposition times of: (a) 30 min, (b) 60 min and (c) 90 min

Figure 4.5. shows that as the current density increases, the layers' thickness increases for all studied systems. Other authors [243-245, 115] have also reported an increase of the layers' thickness with the increase of the applied current density and of the nanoparticles concentration added in the electrolyte.

4.2.2. Influence of current density on current efficiency (η [%])

The current density influence (23 mA/cm², 48 mA/cm² and 72 mA/cm²) applied to the electrodeposition process for obtaining nanocomposite layers in the cobalt matrix on the efficiency deposition (current efficiency) η [%] for the pure Co layer and the Co /nano-CeO₂ nanocomposite layers obtained by adding different nanoparticle concentrations (10, 20 și 30 g/L) and deposition times (30 minutes, 60 minutes, 90 minutes), similar results have been reported by other authors as well [245-246].

4.2.3. Influence of current density on the inclusion degree of CeO₂ nanoparticles in the cobalt matrix

The calculation procedure to determine the inclusion degree of the cerium oxide nanoparticles is summarized in subchapter 4.1.3.

The inclusion degree of the nanoparticles decreases with the increase of the current density for all studied systems. Other authors have also reported that the inclusion degree of nanoparticles decreases with the increase of current density. This behavior is possible because the current density has a considerable effect on the current-potential relation in any electrodeposition process [247-250].

4.3. Partial conclusions

In conclusion, parameters like the current density, the agitation system, the electrolyte's pH, the electrolyte's concentration, and the deposition time have important roles in the electrodeposition quality performance. Thus, in order to obtain conditions of high-quality electrodeposition, these parameters must be studied accordingly. From the data presented in this chapter, we can conclude the following:

From the analysis of the influence of current density and the time on the thickness of the obtained layers measured in cross-section, it can be observed an increase of the layers' thickness with the increase of time and current density, and also with the increase of nanoparticles concentration presented in the deposition electrolyte.

The increase of current density and of time on the current's efficiency had an important role in increasing the values of current efficiency for the studied nanocomposite layers. From the presented data, it can be seen that the pure Co layers, at all current densities and studied times, had lower efficiency values (however over 80%) in contrast with the nanocomposite layers in which different concentrations of nanoparticles were added. In this case for the Co /nano-CeO₂ – 30 g/L system, the efficiency value of the current reaches 98.90%.

From the SEM-EDX analysis, the method by which the inclusion degree of the nanoparticles was calculated, showed that with the increase of the deposition time and the CeO₂ nanoparticles concentration, the inclusion degree of the nanoparticles in the nanocomposite layer increases, but this inclusion degree of nanoparticles decreases for the same studied system with the increase of current density.

CHAPTER V

MORPHOLOGICAL, STRUCTURAL AND TOPOGRAPHIC CHARACTERIZATION

It is more and more acknowledged the fact that nanocomposite or nanostructured hybrid layers represent a series of challenges regarding the characterization of surfaces which have the potential to inhibit or obstruct the scientific and technological impact of surface nanoscience and nanotechnology and, lastly, in order to create the best, it is necessary to study physical, mechanical and chemical modifications that these cause.

This chapter analyses the properties of the nanocomposite layers obtained through classical and advanced characterization methods to highlight the modifications that occur in the surface's morphology and in the obtained layers' structure, the emphases being on characterizing the obtained surfaces with the help of the scanning electron microscopy (SEM-EDZ) from a morphological and compositional, topographical (roughness), mechanical (microhardness), structural (XRD), biological (hydrophobicity analysis by measuring the contact angle) point of view. The chapter ends with partial conclusions of the study.

5.1. Morphological and compositional analysis of the biomaterials' surfaces and electrodeposited layers by electron microscopy (SEM-EDX)

The morphological and compositional analysis (SEM-EDX) of the obtained surfaces was done with the help of the scanning electron microscope described in chapter II (subchapter 2.4) and the EDX specters were acquired with the help of the EDAX Genesis software.

The analysis using SEM electron microscopy highlights the morphological difference of the surfaces with CeO₂ nanoparticles present in the solution, in different concentrations in contrast with the electrodeposited pure metal. The micrographs (SEM) for pure cobalt samples obtained under the same conditions as those for the Co/nano-CeO₂ functional layers show different morphologies. The electrodeposition morphology of the obtained layers differs depending on the applied current density and the amount of CeO₂ nanoparticles in the electrolyte solution. Hence, in figure 5.1. SEM morphologies obtained for pure cobalt layers at 23 mA/cm², 48 mA/cm², 72mA/cm² at the highest time studied, are presented.

From figure 5.1., it can be seen that with the increase of current density applied to the electrodeposition process, the morphology of the pure cobalt modifies. In figure 5.1. (a), for pure Co, it can be seen that the shape of the cobalt crystals is an irregular polyhedral one, and with the increase of current density to 48 mA/cm² (figure 5.1 (b)) it can be observed that these crystals become more prominent. With the increase of current density to 72 mA/cm² (figure 5.1 (c)) it can be observed that the pure cobalt layer displays a branched acicular crystalline structure. Similar behavior regarding the modification of the structures with the increase of current density has been noticed by other authors as well [82, 251].

Furthermore, the SEM morphologies obtained for the Co/nano-CeO₂ (10 g/L, 20 g/L, 30 g/L) layers at 23 mA/cm², 48 mA/cm², 72mA/cm² at the highest time studied, are presented.

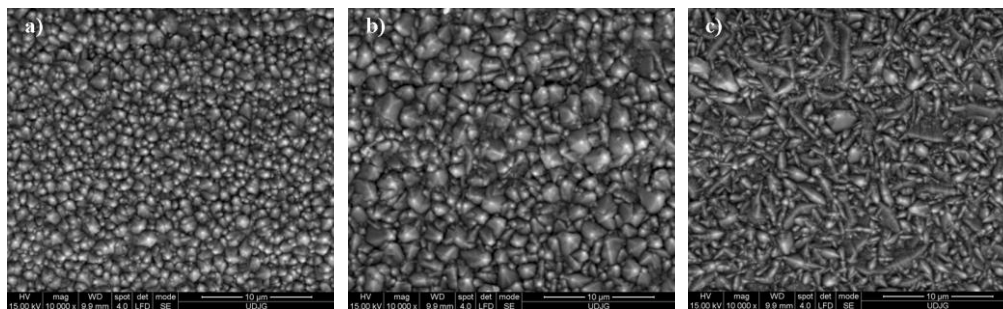


Figure 5.1. SEM morphologies obtained for pure Co layers at: a) current density of 23 mA/cm^2 , b) current density of 48 mA/cm^2 , c) 72 mA/cm^2

We can see that with the presence of the dispersed phase of cerium oxide (10 g/L) in the cobalt matrix, the structures become more homogeneous. It also can be seen that the nanoparticles of cerium oxide also come in small agglomerations and with the increase of current densities the presence of CeO_2 nanoparticles is diminished.

This trend is also confirmed by the inclusion degree of nanoparticles present in obtained layers. In the case of adding 20 g/L CeO_2 nanoparticles it can be observed that the crystalline structures become more homogeneous with the increase of the dispersed phase compared to the layers obtained by adding 10 g/L CeO_2 . It can be noticed that with the increase of the nanoparticle concentration to 30 g/L the inclusion degree of the nanoparticles is visibly higher compared to the $\text{Co/nano-CeO}_2 - 10 \text{ g/L}$ and $\text{Co/nano-CeO}_2 - 20 \text{ g/L}$ layers. At the same time, the disrupting of the increase of cobalt crystals can be caused by a local increase of the pH, induced by the H^+ absorption at the level of dispersed particles which takes place at the level of the adsorption-desorption phenomenon at the cobalt-electrolyte interface [115].

The SEM-EDX compositional analyses correspond to the SEM micrographs. And the main identified elements are Co, O, Ce. Another aspect to be mentioned is that all the samples have been gilded so that is why the peak gold appears in the range of 2.12 keV . It must be mentioned that for the compositional calculation of the EDX specters, the gold was eliminated from the analyzed elements.

It was observed that the cobalt element (Co) displays a signal in two distinct regions on the x-axis between $0.67 \text{ keV} - 0.72 \text{ keV}$ and $6.9 \text{ keV} - 7.66 \text{ keV}$. It can also be noticed that the Co peaks' intensity raises with the increase of current intensity, but it maintains the signals' position from the two regions previously mentioned, for the $\text{Co/nano-CeO}_2 - 10 \text{ g/L}$ layers obtained at the current densities of $23, 48, 72 \text{ mA/cm}^2$. We can see that in the case of the $\text{Co/nano-CeO}_2 - 10 \text{ g/L}$ layers, the Co element keeps the two regions distinct, unchanging as a position in the case of the nanocomposite layers. We notice the appearance of the O element in the signal region of 0.523 keV and the appearance of the Ce element which displays signals between the $4.73 - 6.64 \text{ keV}$ region. The cerium element can also be seen. At the current density of 23 mA/cm^2 it is present in a mass percentage of 5.55% , while for the current density of 48 mA/cm^2 the presence of the Ce element decreases compared to the current density of 23 mA/cm^2 at a mass percentage of 3.79% , and in the case of the current density of 72 mA/cm^2 this value of wt. for Ce decreases even more to a value of 2.73% . The increase of the oxygen element with the increase of the current density does not coincide with the decrease of the cerium element because this behavior has been explained in the specialized literature as being possible due to the oxidation of active metals, cobalt, during the electrochemical reduction process with increasing current density [252-254].

In the case of $\text{Co/nano-CeO}_2 - 20 \text{ g/L}$ layers obtained at the three current densities, the inclusion process of the cerium elements increases for all current densities in contrast with those obtained by adding 10 g/L CeO_2 . However, in case the same CeO_2 nanoparticles concentration of 20 g/L is kept, it can be noticed a decrease of the cerium element with the increase of the current density.

It can be observed that the cerium element, in the case of layers where 30 g/L of CeO_2 nanoparticles were added, is present in the highest mass percentage at all studied current densities compared with the $\text{Co/nano-CeO}_2 - 20 \text{ g/L}$ and $\text{Co/nano-CeO}_2 - 10 \text{ g/L}$ layers. This is due to the increase in the dispersed phase concentration from the deposition electrolyte, but keeping the same descending trend of the inclusion mass percentage of the cerium element with the increase of current

density. This behavior is consistent with the results obtained by other researchers [247-250].

5.2. Roughness analysis

The roughness analysis was done with the device described in chapter II, average roughness values (R_a) were analysed depending on the current density (23, 48, 72 mA) and the deposition time (30, 60, 90 min).

From the obtained analysis data of roughness, we can conclude that the roughness of the studied surfaces increases with time, current density and the increase of nanoparticle concentration.

5.3. Structural characterization by X-ray diffraction (XRD)

In order to identify crystalline phases as well as to estimate the dimensions of the crystal compounds, formed on the pure Co studied surfaces, compared to the Co/nano-CeO₂ nanocomposite layers, depending on the current density at the highest studied time, the X-ray diffraction (XRD) analysis was performed, using the device described in chapter II. The XRD specters are presented, obtained at the current density of 23, 48, 72 mA/cm² for pure Co layers compared with the Co/nano-CeO₂ systems, electrochemically obtained by adding a three nanoparticle concentration (10 g/L, 20 g/L, 30 g/L).

Therefore, including CeO₂ nanoparticles in the cobalt matrix leads to nanostructuring the cobalt matrix by reducing the sizes of cobalt crystallites.

Increasing the current density in the case of pure cobalt deposition leads to increasing the sizes of cobalt crystallites from the electrodeposited layer, while for the nanocomposite layers, the crystallites' size decreases with the increase of the current density which confirms the nanostructuring effect of the nano-CeO₂ particles electrodeposited with the cobalt.

Including CeO₂ nanoparticles in the cobalt matrix disrupts its preferential crystallization as well.

5.4. Microhardness analysis of layers

The Vickers microhardness tests on the obtained layer have been carried out with the help of the device described in chapter II, subchapter 2.7., according with the ASTM E-384-C1327 standard [286].

From the microhardness analysis of the nanocomposite layers, it can be noticed an increase of the microhardness values with the increase of the CeO₂ nanoparticles content in the deposition electrolyte, being almost constant with the increase of the deposition time. Improving the hardness of Co / nano-CeO₂ nanocomposite hybrid layers is related to the strengthening effect caused by the dispersion of CeO₂ nanoparticles embedded in the layers which block the dislocations' movement in the cobalt metallic matrix. G. CÂRÂC and her team [287] observed an increase of the layers' microhardness with increasing concentration of the dispersed phase (Al₂O₃ nanoparticles) in nickel matrix obtained by the electrodeposition method.

5.5. Hydrophobicity characterization of surfaces

Therefore, the wetting of the surfaces for this study was determined with the help of the contact angle method (sessile drop) using a drop of the Hank biological solution (10 μ L) described in chapter II as well. The average values of the measurements on different coating were made depending on the current density and the time required for the electrodeposition process.

From the hydrophobicity analysis we can say that the values of the contact angle decrease with the increase of time, current density, as well as the concentration of nanoparticles.

This decrease of the contact angle's values is consistent with the values' increase obtained in



studying the roughness supported by the Wenzel equation.

$$\cos\theta_w = r \cos\theta_y \quad (5.2)$$

Where r is the average roughness, θ_w is the value of the measured contact angle, θ_y is the value of the Young contact angle on an ideal smooth surface [280, 288-289].

This equation shows that the increased roughness reduces the contact angle, which means that a more hydrophilic surface appears.

5.6. Partial conclusions

From this chapter, entitled morphological, topographic and structural characterization of surfaces obtained by the electrodeposition methods of CeO₂ nanoparticles in cobalt matrix on a 304L stainless steel sublayer, found in this study under the name of (pure Co, Co /nano-CeO₂ – 10 g/L, Co /nano-CeO₂ – 20 g/L and Co /nano-CeO₂ – 30 g/L), we can conclude that:

From the SEM-EDX analysis of the nanocomposite functional layers, it can be observed that for pure Co the size of the cobalt crystals is inclined to increase with the increase of current density, and when adding cerium oxide nanoparticles, they change their morphology and the crystals' size tend to decrease. Concurrently, for the functional layers with added cerium oxide nanoparticles, it can be noticed that with the increase of current density the layers' evenness is better.

The EDX analysis confirms the presence of CeO₂ nanoparticles in the obtained layers, at the same time it is noticeable that the inclusion degree of the studied nanoparticles decreases with the increase of the current density.

From the roughness analysis of the obtained layers, it can be noted an increase of the layers' roughness with the increase of current density and with the time required for the electrodeposition process.

From the layers' microhardness analysis, it can also be detected an increase of the microhardness values with time, the current density applied to the process of obtaining functional layers and the increase of CeO₂ nanoparticles concentration.

From the contact angle's analysis it can be noted that with the increase of time, the increase of nanoparticles concentration, and of current density, the surfaces become more hydrophilic indicating that from a biological point of view this behavior leads to a better osseointegration of the possible implant.

From the XRD analysis, it can be said that CeO₂ nanoparticles incorporated in the Co matrix disturb the preferential orientation of the cobalt layer, at the same time decreasing in intensity the corresponding peak to the pure Co layer.

Including CeO₂ nanoparticles in the cobalt matrix leads to the nanostructuring of the cobalt matrix by decreasing the cobalt crystallites' dimensions.

The increase of current density in the case of pure cobalt deposition leads to the increase of the cobalt crystallites' dimensions from the electrodeposited layer, while for the nanocomposite layers the crystallites' dimension decreases with the increase of the current density, which confirms the nanostructuring effect of the nano-CeO₂ particles electrodeposited with the cobalt.

CHAPTER VI

STUDY OF TRIBOCORROSION RESISTANCE (CORROSION AND WEAR) OF OBTAINED BIOMATERIALS AND FUNCTIONAL LAYERS

The necessity of selecting or designing new surfaces for future biomaterials, as well as minimizing the service costs and extending the lifespan of the existent biomaterials has led to the necessity of a better understanding of the process of surface degradation, especially when some parts of the human body are subjected to the tribocorrosive process. This gave birth to the active research area named tribocorrosion, which tries to approach the previously mentioned problems and to understand the mechanism of surface degradation when mechanical wear and chemical / electrochemical processes interact between them. In this chapter, the tribocorrosive behavior of the used support for co-deposition, i.e. the 304L stainless steel support layer, the functional layers obtained by electrodeposition of CeO₂ nanoparticles in the cobalt matrix compared to the pure Co layer without adding the nanoparticles obtained at the current density of 23 mA/cm² (because the inclusion degree of the nanoparticles was much higher), have been monitored and evaluated by electrochemical and wear measurements (three applied forces: 1N, 3N and 5N, at a constant speed of 120 rpm and with a duration of 5000 cycles) in the Hank biological solution at room temperature with the help of a modified tribometer described in chapter II. Electrochemical measurements were used, like OCP, EIS for characterizing the behavior to corrosion of the 304L stainless steel and of the functional layers. The morphological analysis, after carrying out the wear tests, was done with the help of SEM and the optical profilometry was used to determine the total wear volume at the end of the wear tests.

6.1. Tribocorrosion of the 304L stainless steel

In this part, the 304L stainless steel, which was used as support layer for the obtained Co/nano-CeO₂ nanocomposite layers by the electrodeposition method, is tested for tribocorrosion in the same biological solution and with the same parameters as the nanocomposite layers. This stainless steel is a material frequently used in the biomedical field, especially in different structures of dental medicine. Tribocorrosive aspects of the 304L stainless steel in the Ringer biological solution were studied by another way of arranging the sample and another way of friction, bidirectional friction, with 200 μm amplitude [138, 290].

In these tribocorrosive tests, the unidirectional pin-on-disk method was used, described in chapter 2.

6.1.1. Evaluation of electrochemical parameters

6.1.1.1. Open circuit potential (OCP)

In figure 6.1. the open circuit potential of the 304L stainless steel is presented, for the tribocorrosion test by applying a force of 3N where it can be observed the open circuit potential at the sample immersion in the biological solution, before applying the friction force, during the friction,



after lifting the friction force, and stopping the friction.

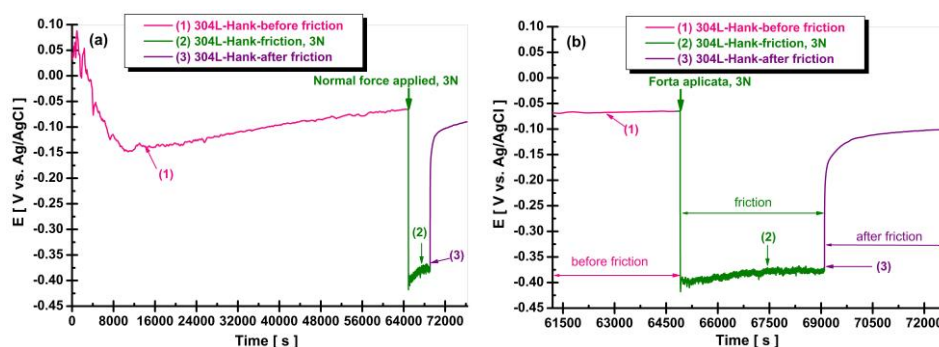


Figure 6.1. Variation of the open circuit potential for the 304L stainless steel in the Hank biological solution: (1) during the immersion, before applying the friction force; (2) during the application of the frictional force, and the friction to the normal force applied of 3N, (3) after lifting the force, and stopping the friction; (a) the entire tribocorrosive test period (before, with friction, after friction); (b) zoom in the open circuit potential where the 3N force was applied

Figure 6.1. shows that at the beginning of the test, when submerging the sample in the solution, before the 3N force is applied, the potential's value starts from 37.51 mV vs. Ag/AgCl, value which has a slight shift towards negative values for approximately 4 h until the potential of -14.86 mV vs. Ag/AgCl. After 4 h, the potential shifts towards more positive values (nobler), getting at the end of the 18 h to a potential value of approx. -6.5 mV vs. Ag/AgCl. A shift of the potential to nobler values, before applying the normal force, indicates passivation of the material during immersion in the solution. When the normal force was applied, it can be noticed a sudden shift of the potential towards negative values, in the cathodic field reaching to a value of -410.34 mV. The potential difference of this shift being large of $\Delta E = 372.83$ mV, which indicates degradation of the material in the wear area by removing the passive film from the surface of the 304L stainless steel in the Hank biological solution, the respective area becoming active to the corrosion process.

During friction the potential remains in this cathodic zone, actually having a slight upward trend, $\Delta E = 12.95$ mV, until the friction force is stopped, which confirms the fact that after the rubber, the surface of the stainless steel has a tendency to repassivate (to recover the passive film).

After stopping applying the 3N force, it can be seen a sudden shift of the potential towards nobler values, getting to the end of the measurement to a potential of -90.75 mV vs. Ag/AgCl, which is approximately 33.88 mV more negative than the value of the passivated stainless steel surface potential before applying friction $E = -6.5$ mV. This behavior reveals the capacity of repassivation of the steel's surface in the area of the wear trace, but also a degradation in the wear trace area which can not return to its initial state.

6.1.1.2. Electrochemical impedance spectroscopy (EIS)

The electrochemical impedance spectroscopy (EIS) is the most sophisticated technique among the electrochemical methods in this study, being imposed to characterize the reactivity and polarization resistance of the 304L stainless steel in the Hank biological fluid. For the EIS, a variation of the 10 mV sinusoidal signal was imposed versus the OCP at frequencies from 10^4 Hz to 10^{-3} Hz, 10 frequencies per decade, registered before the friction tests, during friction, and after stopping the friction at different applied charges (3N, 5N). The rotation speed was chosen to 120 rpm and the total number of rotations for each test was established at 5000 cycles.

6.1.2. Evaluation of mechanical parameters, friction coefficient

The coefficient of friction (COF) is a number without dimensions, which is defined as the report



between the tangential force that opposes the friction and the normal force applied [298].

The coefficient of friction (COF) recorded during pin-on-disk friction (slipping) record simultaneously with the open potential circuit during friction, and the impedance during friction, is presented. The average coefficient of friction was calculated for both forces, from the values recorded from the balance state during the friction test in the corrosive environment of the Hank biological solution.

It can be noted an increase in the friction coefficient of the 304L stainless steel with the increase of the applied normal force. The average value of the friction coefficient for the 304L stainless steel at the applied force of 3N has a value of 0.367, and for the applied force of 5N this value increases to 0.709. Similar results in terms of increasing the coefficient of friction with increasing charges have been reported by other authors as well [244].

6.1.3. 2D and 3D profile of the wear trace. Wear volume loss in the trace

The wear volume was determined by using a microtopograph, STIL (France), with a high resolution, equipped with fiber optic for capturing the light signal and analyzing its intensity with a lateral resolution of 1 μm and a vertical resolution of 30 nm. Then, the image is transformed in a surface with 2D and 3D profile with the help of the MountainsMap Universal software application. The total wear volume for each sample was determined by measuring the 3D profile corresponding to traces of wear at four distinct points. From the 4 points of the 3D wear profile, evenly distributed, the local volume due to material loss by wear (w) was calculated. The average value of the resulting wear loss is multiplied by the length of the wear trace (L) to obtain the total loss of wear volume over the entire wear trace (Wt). Loss of the volume material in the wear trace was smaller for the 304L stainless less submerged in the Hank solution, at the applied normal charge of 3N ($3.32 \cdot 10^{-6} \mu\text{m}^3$) in contrast with the 304L stainless less submerged in the Hank solution subjected to the application of a 5N normal force ($4.62 \cdot 10^{-6} \mu\text{m}^3$). This behavior indicated the fact that with the increase of the applied normal force in the tribocorrosive test, the material's degradation is stronger.

6.1.4. SEM morphological analysis of the wear trace

The surface morphologies of the 304L stainless steel, after continuous friction by unidirectional slipping at different F_n at 3 N and 5 N in the Hank biological solution, were obtained using SEM. The width of the wear trace for the 304L stainless steel submerged in the Hank solution obtained after the friction tests at F_n of 3 N is 464.92 μm , while the width of the wear trace for the same studied material, but at F_n of 5 N, is much higher of approximately 482.63 μm .

From the results obtained in studying the tribocorrosion of uncoated 304L stainless steel, previously presented, we can conclude the necessity of using modification methods of surfaces with the purpose of improving the behavior to tribocorrosion of the 304L stainless steel, and last but not least, to increase the lifespan in terms of using it in applications with biomedical potential.

6.2. Co/nano-CeO₂ functional layers

6.2.1. Evaluation of electrochemical parameters

6.2.1.1. Open circuit potential (OCP)

The first stage of the testing protocol to tribocorrosion [110] is measuring the electrochemical behavior of the obtained functional layers, submerged in the Hank biological solution. The open circuit potential evolution was monitored for 18 hours before applying the applied normal forces (1N-5N) of the obtained Co/nano-CeO₂ nanocomposite layers.



Time is an essential parameter to observe the attainment of a balance state in the Hank solution because it is an important feature of the passivation process.

If we want to compare this shift of the potential towards more negative values, thus towards values of the potential in the active field for all the surfaces of the studied materials, when the mechanical disruption by friction in the corrosive environment is applied, a schematization is displayed in figure 6.14.

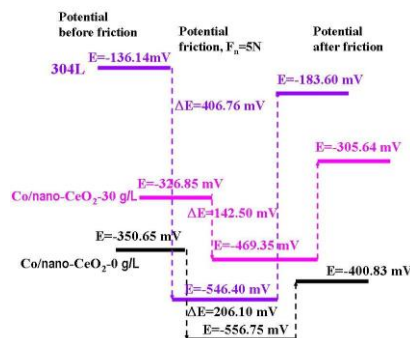


Figure 6.14. Schematic representation of the potential shift when applying and stopping the normal friction force of 5N for the 304L stainless steel support, and for the electrodeposited layers of pure Co and Co/nano-CeO₂-30g/L nanocomposite

As figure 6.14. shows, the biggest potential shift when applying the friction force of 5N is registered at the 304L stainless steel, $\Delta E=406.706$ mV, which confirms that is the most sensible to degradation by friction in corrosive environment, namely the most sensible to tribocorrosion (simultaneous corrosion and wear). Moreover, the 304L stainless steel can no longer reach the initial value of the passive potential recorded before friction, confirming the irreversible modifications of its surface degradation in these conditions.

The least affected of the tribocorrosive degradation process is the Co/nano-CeO₂ - 30 g/L nanocomposite whose potential, when starting the friction force of 5N, shifts towards more negative values (active) just with $\Delta E=142.50$ mV. Also, the repassivation potential of the nanocomposite surface, after stopping the force, reaches even more positive values (noble), than the initial value recorded before starting the friction force. We can say that friction highlights more CeO₂ nanoparticles on the surface of the nanocomposite, as it will be highlighted by the analysis of friction traces.

6.2.1.2. Electrochemical impedance spectroscopy at the open potential (EIS)

If the first stage in evaluating the electrochemical parameters in the study of tribocorrosion is evaluating the open circuit potential, the method which shows the material's passivation / repassivation tendency, a second stage in the experimental protocol is plotting the EIS diagrams (before, during and after friction) to the open potential, in the frequency range from 10⁴ Hz to 10⁻³ Hz, at the normal applied force of 5N, and 10 frequencies / decade, with the purpose of evaluating the polarization resistance of the studied surfaces before friction, during friction, and after friction in the Hank biological solution. For interpreting the data, the Z_{view} software was used, and for mathematical simulation of the experimental data, the simple equivalent circuit was used.

The polarization resistance for the nanocomposite layers with CeO₂ nanoparticles is much bigger in contrast with the polarization resistance for the pure Co layer.

For a better overview of the polarization resistance results obtained from the EIS diagrams, before frictions, during friction, and after friction, modeled and simulated using the equivalent circuit, figure 6.16. presents these values of the polarization resistance in the form of graphs on columns.

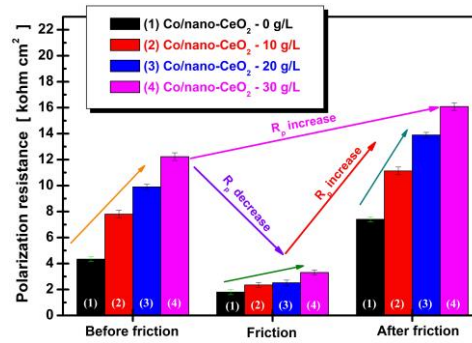


Figure 6.16. Polarization resistance obtained from the EIS experimental data simulation, obtained for the pure cobalt and studied nanocomposite layers, before friction, during friction, and after friction, tested in the Hank biological solution at the applied normal force of 5N:
 (1) pure Co, (2) Co /nano-CeO₂ – 10 g/L, (3) Co /nano-CeO₂ – 20 g/L and
 (4) Co /nano-CeO₂ – 30 g/L

From figure 6.16. it can be noticed that before the friction tests, the polarization resistance, R_p , for the pure Co layer has a value of 4.3 kΩ cm², for the Co /nano-CeO₂ – 10 g/L layer this value increases to 7.8 kΩ cm², for 20 g/L CeO₂, $R_p = 9.9$ kΩ cm², while for the maximum concentration of CeO₂ studied this R_p reaches the highest value of 12.230 kΩ cm².

6.2.2. Evaluation of mechanical parameters, friction coefficient

The Co/nano-CeO₂ layers display a lower coefficient of friction than the pure Co layer, and at the same time it can be noticed that the coefficient value decreases with the increase of the CeO₂ nanoparticles concentration.

For the pure cobalt, we see an average value of the friction coefficient of approximately 0,326, for Co /nano-CeO₂ – 10 g/L an average value of 0.236, for Co /nano-CeO₂ – 20 g/L an average value of 0.228, reaching for the surface with 30g/L CeO₂ nanoparticles a valued of 0,175. These results prove a good incorporation effect of the cerium oxide nanoparticles in the cobalt matrix. It seems that CeO₂ nanoparticles have the capacity to eliminate the adhesive effects between the counterweight and the surface of the layer, thus reducing the coefficient of friction.

Similar behavior regarding the decrease of the friction coefficient with the increase of the nanoparticles concentration has been reported by other authors, as well, in the specialized literature [301-302]. The same tendency was seen in the case of the applied forces of 1 and 3N, but the friction coefficient values were bigger with the decrease of the charge applied to the process.

6.2.3. 2D and 3D profile of the wear trace.

Wear volume loss in the trace depending on the applied normal force

The volume loss results in the wear trace of the pure cobalt layer, and of the Co/nano-CeO₂ nanocomposite layers calculated according to the applied normal forces of 1, 3 and 5 N, are presented in fig. 6.19.

From figure 6.19. it can be stated that the wear volume loss from the wear traces of all layers increases with the increase of the applied normal force. Increasing the content of the dispersed cerium oxide in the cobalt's deposition electrolyte, the material's loss volume from the wear traces of the nanocomposite layers has a downward trend than those wear traces of the pure cobalt layer at all applied normal forces. This behavior confirms once more the performance improvement to tribocorrosion by incorporating CeO₂ nanoparticles in the cobalt matrix under lubricating conditions.

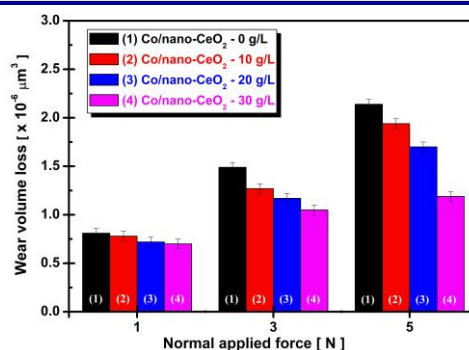


Figure 6.19. Loss of volume calculated from each wear trace after tribocorrosive investigations in the Hank biological solution of the pure cobalt layers, compared with the Co/nano- CeO_2 nanocomposite [116]

6.2.4. Comparative analysis of wear traces of nanocomposite layers and the 304L stainless steel

For a comparative evaluation of the behavior in tribocorrosive conditions, figure 6.20. shows the material loss in the wear trace both for the 304L stainless steel support material, and for the electrodeposited layers of pure cobalt, and Co/nano- CeO_2 (10, 20, 30 g/L) nanocomposite layers, resulted from the tribocorrosion test in the Hank biological solution by friction with an applied normal force of 5N.

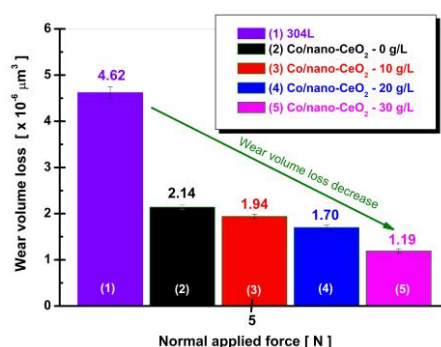


Figure 6.20. The wear volume loss from the wear trace by the tribocorrosive effect in the Hank biological solution when applying a normal friction force of 5N: (1) 304L stainless steel; (2) pure Co; (3) Co/nano- CeO_2 - 10 g/L, (4) Co/nano- CeO_2 - 20 g/L, (5) Co/nano- CeO_2 - 30 g/L

It can be seen in figure 6.20. that the biggest loss of material in the wear trace is suffered by the 304L stainless steel by applying a friction force of 5N in the corrosive environment of the Hank biological solution. This confirms that the 304L stainless steel is the most affected by the tribocorrosion degradation process (corrosion and wear) in the Hank biological environment. Among the electrodeposited layers on the 304L stainless steel support, the most resistant to the tribocorrosion process is the Co/nano- CeO_2 -30 g/L nanocomposite layer which has the lowest material loss in the wear trace. This behavior is due to the stiffening effect of the CeO_2 nanoparticles, as well as their nanostructuring effect by incorporating them in the cobalt matrix.

6.2.5. SEM morphological analysis of the wear trace

After the tribocorrosion tests, the samples' surfaces were analyzed with the help of the electron microscopy (SEM). SEM micrographs of the wear traces are presented, after continuous friction - 5000 cycles of the pin with an applied force of 5N on the layers' surface.

From figure 6.21. it can be distinguished that the width of the wear traces for the nanocomposite layers significantly decreases with the increase of the CeO₂ nanoparticles concentration. For the pure Co layer, it can be noticed that the width of the wear trace is 460 μm, while for the CeO₂ 10 g/L nanoparticles layer the width of the wear trace decreases to 397 μm, reaching the highest concentration studied of 378 μm.

This demonstrates that, without incorporating the CeO₂ nanoparticles in the Co matrix, the wear resistance of the pure Co layer is quite weak.

It can be concluded that incorporating the CeO₂ nanoparticles in the cobalt matrix can largely reduce the wear of the nanocomposite layers in the cobalt matrix, additionally, the wear resistance of the Co/nano-CeO₂ nanocomposite layer is improved, in contrast with the pure Co layer without the nanoparticle addition.

Since CeO₂ nanoparticles ensure both dispersion consolidation, as well as a good effect on the corrosion behavior, highlighted by the EIS diagrams resulted before friction, during friction, as well as after stopping the friction, and the improvement of the tribological behavior, it results that the performances to tribocorrosion of the Co/ nano-CeO₂ nanocomposite layers are superior both to pure cobalt layers and as well to the 304L stainless steel support.

6.3. Partial conclusions

To investigate the tribocorrosive behavior in the Hank biological solution of the functional layers obtained in this study, both in-situ electrochemical investigation (OCP, EIS) methods, in-situ friction coefficient measurement (COF), and ex-situ methods were used to characterize the wear traces.

From the open circuit potential before friction, it can be observed a shift of the potential towards nobler values (positive) for the Co/nano-CeO₂ nanocomposite layers in the Hank biological solution, in comparison with the pure Co layer.

When the normal force of 5N is applied, the open potential variation leads to a shift towards more negative values (active) of the pure cobalt layer, in comparison with those of the nanocomposite layers which are positive during friction. After stopping the friction force, it was seen that the nanocomposite layers repassivate faster, reaching the passive state after stopping the wear tests, even at more positive potentials than the potentials recorded before friction.

Electrochemical impedance spectroscopy measurements before, during, and after friction showed better behavior for the Co / nano-CeO₂ layers, with R_p values increasing as the concentration of nanoparticles present in the electrolyte increased when subjected to a process of tribocorrosion in Hank biological solution, compared to the pure Co layer.

From the SEM micrographs, it can be distinguished that the width of the wear trace for the nanocomposite layers decrease significantly with the increase of the CeO₂ nanoparticles concentration.

At the same time, the Co/nano-CeO₂ nanocomposite layers present an increased wear resistance, demonstrated by lower friction coefficients, including a small loss of the wear volume in contrast with the pure Co layer.

Increasing the applied normal force affects the surfaces' degradation during the friction trials by continuous unidirectional sliding for the studied layers.

Thus, the need to use surface modification methods can be emphasized with the purpose of improving the behavior to tribocorrosion of the 304L stainless steel, and last but not least, to increase the lifespan, in order to use it in applications with biomedical potential.

CHAPTER VII

GENERAL CONCLUSIONS, FUTURE PERSPECTIVES

7.1. General conclusions

In the last years, there was a general necessity to develop new biomaterials that can be inserted in the human body without causing side effects. Consequently, the objective of this study is to improve the 304L stainless steel surface by the electrodeposition techniques in the cobalt metallic matrix using, as dispersed phase, cerium oxide nanoparticles with different concentrations in order to improve the tribological performances in the Hank biological solution. Principally, this study aimed to evaluate the possibilities of this new nanomaterial candidate for biomedical applications, as well as obtaining a better understanding of the tribocorrosive behavior in an environment which simulates the human body fluid, namely the blood (Hank).

From the analysis of chapter I, we can conclude that one of the most advanced methods of modifying the surfaces is **electrodeposition** which is assimilated with the **bottom-up method of nanotechnology**.

The most important factors that influence the deposition of functional layers are the current density, time, the concentration of particles, the nanoparticles' dimension, the electrolyte's composition, the electrolyte's pH, and agitation speed.

Starting from the fact that the most economically / qualitatively profitable method was identified, as well as the materials necessary for the development of the experimental plan, the obtained results have an innovative character.

The first step was studying the kinetics and mechanism of obtaining functional layers by electrodeposition. The cobalt's electrodeposition from an electrolyte bath, to which different concentrations of CeO₂ nanoparticles were added, was studied at different cathodic potentials (vs. Ag/AgCl) by the following methods: cyclic voltammetry (CV), electrochemical impedance spectroscopy (EIS), chronocoulometry and chronoamperometry.

The cyclic voltammetry study showed that by adding CeO₂ nanoparticles in the solution leads to a shift of the cobalt's reduction curve towards more positive potential values with the increase of the nanoparticles concentration in the electrolyte, thus affecting the nucleation and growth mechanism of the cobalt matrix.

The electrochemical impedance specters are influenced by the addition of CeO₂ nanoparticles, and therefore, the charge transfer resistance decreases in contrast with the pure Co system. By increasing the CeO₂ nanoparticles concentration, the reduction of the cobalt is active, the ionic transport is improved, as well as the density of the nucleation sites.

The chronocoulometry curves of the pure Co and the Co/nano- CeO₂ systems emphasize an increase of the current density with the increase of the CeO₂ nanoparticles concentration, due to the increase of the active surface.

After studying the kinetics and the mechanism of obtaining the layers, the next step was the influence study of the electrochemical parameters for obtaining the functional layers on the properties of the obtained layers.

The analysis of the influence of current density and time on the obtained layers' thickness measured in cross-section, shows an increase of the layers' thickness with the increase of time, and current density, as well as with the increase of the nanoparticles concentration present in the deposition electrolyte.

The increase of the current density and of the time on the current's efficiency had an important role on increasing the percentage values of the current efficiency for the studied nanocomposite layers.



The presented data show that the pure Co layers at all current densities and studied times, the efficiency percentage values were lower (however over 80%), compared to the nanocomposite layers in which different concentrations of nanoparticles were added.

In the electrodeposition case for the Co /nano-CeO₂ – 30 g/L system, the current's efficiency value reaches 98.90%.

The SEM-EDX analysis, method by which the nanoparticles' inclusion degree was calculated, showed that with the increase of the deposition time and the CeO₂ nanoparticles concentration, the inclusion degree of the nanoparticles present in the layer increases, but this inclusion degree of the nanoparticles decreases for the same studied system with the increase of current density.

From the morphological, topographic and structural characterization of surfaces obtained by the electrodeposition methods of CeO₂ nanoparticles in cobalt matrix on a 304L stainless steel sublayer, found in this study under the name of (pure Co, Co /nano-CeO₂ – 10 g/L, Co /nano-CeO₂ – 20 g/L and Co /nano-CeO₂ – 30 g/L), we can conclude that:

The SEM-EDX analysis of the nanocomposite functional layers states that for pure Co the size of the cobalt crystals is inclined to increase with the increase of current density, and when adding cerium oxide nanoparticles, they change their morphology and the crystals' size tend to decrease.

Concurrently, for the functional layers with added cerium oxide nanoparticles, it can be noticed that with the increase of current density, the layers' evenness is better.

This also proves the nanostructuring effect of the CeO₂ particles that stiffen the cobalt matrix by their electrodeposition with cobalt, an effect observed in X-ray investigations of the structure (XRD).

The EDX analysis confirms the presence of CeO₂ nanoparticles in the obtained layers, and at the same time it is noticeable that the inclusion degree of the studied nanoparticles decreases with the increase of the current density.

The roughness analysis of the obtained layers exhibits an increase of the layers' roughness with the increase of current density, and with the time required for the electrodeposition process.

The layers' microhardness analysis displays an increase of the microhardness' values with time, and with the current density applied to the process of obtaining functional layers.

The contact angle's analysis indicates that with the increase of time, the increase of nanoparticles concentration, and of the current density, the surfaces become more hydrophilic indicating that, from a biological point of view, this behavior leads to a better osseointegration of the possible implant.

The XRD analysis states that CeO₂ nanoparticles incorporated in the Co matrix disturb the preferential orientation of the cobalt layer, at the same time decreasing in intensity the corresponding peak to the pure Co layer with the increase of the dispersed phase concentration (CeO₂ nanoparticles).

From studying the tribocorrosion resistance (corrosion and wear) of the obtained functional layers, we can underline the following:

The open circuit potential before friction, presents a shift of the potential towards nobler values (positive) for the Co/nano-CeO₂ nanocomposite layers in the Hank biological solution, in comparison with the pure Co layer.

When the normal force of 5N is applied, the open potential variation leads to a shift towards more negative values (active) of the pure cobalt layer, in comparison with those of the nanocomposite layers which are positive during friction.

After stopping the friction force, it was seen that the nanocomposite layers repassivate faster, reaching the passive state after stopping the wear tests.

Electrochemical impedance spectroscopy measurements before, during, and after friction showed better behavior for the Co / nano-CeO₂ layers, with R_p values increasing, as the concentration of nanoparticles present in the electrolyte increased when subjected to a process of tribocorrosion in Hank biological solution compared to the pure Co layer.

From the SEM micrographs, it can be distinguished that the width of the wear trace, for the nanocomposite layers, decreases significantly with the increase of the CeO₂ nanoparticles concentration.

At the same time, the Co/nano-CeO₂ nanocomposite layers present an increased wear resistance, demonstrated by lower friction coefficients, including a small loss of the wear volume in contrast with the pure Co layer.

Increasing the applied normal force affects the surfaces' degradation during the friction trials by



continuous unidirectional sliding for the studied layers.

The results obtained from studying the tribocorrosion of the uncoated 304L stainless steel, presented in this chapter, we can underline the necessity for using modification methods for surfaces with the purpose of improving the tribocorrosive behavior of the 304L stainless steel, and last but not least, in increasing the lifespan, in order to use it in applications with biomedical potential.

7.2. Future perspectives

The tribocorrosion behavior of biomaterials, that have undergone surface modifications, can be complicated but at the same time an interesting process. Even though the results of this study are useful for understanding and developing / improving the surfaces of metallic biomaterials (by the electrodeposition method with the purpose of expanding their lifespan regarding the tribocorrosion behavior in environments which simulate the fluids of the human body), studies can continue in the following directions:

Studies regarding the corrosion and tribocorrosion behavior of obtained layers in different biological solutions at human body temperature, by adding proteins (albumin), H₂O₂, lactic acid, hyaluronic acid, etc., in order to see their influence on the resistance of the obtained layers.

Selecting a range of average and big forces for the wear and corrosion tests with the purpose to simulate the human body's biomechanics.

Additional studies regarding the microbiological activity of the obtained layers, as well as the possibility of vivo testing of the obtained functional layers.

Developing new layers on other types of metallic biomaterials, like titanium alloys, and testing them from a biological, mechanical, electrochemical point of view.

The studies may also continue on identifying other methods of obtaining functional layers for improving corrosion and tribocorrosion behavior.

Furthermore, additional investigations of the effect of different methods of surface modification on corrosion and tribocorrosion behavior of Co/nano-CeO₂ layers, and not only, in various mechanical stress conditions that are also important to guide the use of biomedical implants.

CHAPTER VIII

OWN CONTRIBUTIONS AND IMPACT OF THE RESEARCH RESULTS

8.1. Personal contributions

For this study, a bibliographic study of the most recent national and international research regarding the nanocomposite hybrid layers has been carried out with possible biomedical applications in tribocorrosive, corrosive, etc. systems.

Identifying the most profitable methods of modifying the biomaterials' surfaces, as well as finding the best techniques and methods for preparing the support layer, in order to obtain the functional layers.

Preparing the electrolytes used in this study.

Optimizing the working parameters, in order to obtain nanocomposite hybrid layers.

Studying kinetics and the mechanism for obtaining functional layers by electrodeposition in the presence and absence of CeO₂ nanometric dispersed phases in the cobalt matrix.

The influence of the electrochemical parameters for obtaining the functional layers on their properties (the influence of current density and time applied to the process).

Studying the morphological, structural, and topographical (SEM-EDX, XRD, roughness, microhardness, and evaluating the wetting properties of the obtained layers) characterization.

The most important, original contribution is observing the nanostructuring effect of the CeO₂ nanoparticles on the cobalt matrix when they are electrodeposited. Their inclusion in the cobalt leads to a decrease in the size of cobalt crystallites which is emphasized with the increase of the current density.

Studying the tribocorrosion resistance (corrosion and wear) of biomaterials and functional layers obtained in-situ: evaluating the electrochemical parameters, evaluating the mechanical parameters, coefficient of friction, and applying ex-situ methods for characterizing the wear traces.

Schematic representation of all equipment and electrochemical cells used.

Computer control of the performed experiments, data collection from the data acquisition software, interpreting them, and graphical representation.

8.2. Scientific achievements in the field of the research subject

8.2.1. ISI Publications (Clarivate Analytics) - 3

1) Lidia Benea, **Nicoleta Simionescu**, Jean Pierre Celis, **Electro-codeposition of CeO₂ nanoparticles into cobalt matrix to improve the tribocorrosion performances of Co/nano CeO₂ composite layers in biological solution for medical applications**, *Journal of the Mechanical Behavior of Biomedical Materials*, Volume 101, January 2020, 103443. <https://doi.org/10.1016/j.jmbbm.2019.103443>. Impact Factor = 3.485, Q1
Accession Number: WOS:000502881800029

2) **Simionescu Nicoleta**, RavoIU Anca, Lidia Benea, **Electrochemical in vitro Properties of 316L Stainless Steel for Orthodontic Applications**, *Revista de Chimie*, 2019, Vol. 70, Issue 4, p. 1144-1148. Impact Factor = 1.605, Q3, <https://doi.org/10.37358/RC.19.4.7081>, Q3
Accession Number: WOS:000469387200008



3) Lidia Benea, Laurentiu Mardare, **Nicoleta Simionescu**, **Anticorrosion performances of modified polymeric coatings on E32 naval steel in sea water**, *Progress in Organic Coatings*, 2018, vol 123, p. 120-127. Impact Factor = 3.420, Q1, <https://doi.org/10.1016/j.porgcoat.2018.06.020>
Accession Number: WOS:000444357000013

8.2.2. ISI Proceeding Volume Publications - 6

1) **N Simionescu**, L Benea, J P Celis, **Wear-Corrosion Response of Cerium Oxide Reinforced Cobalt Hybrid Composite Layers in Biological Solution**, IOP Conf. Ser.: Mater. Sci. Eng. 572 (2019) 012003. <https://iopscience.iop.org/article/10.1088/1757-899X/572/1/012003/pdf>
DOI:10.1088/1757-899X/572/1/012003.

2) L Benea , **N Simionescu**, **Corrosion Behavior of Ni/WC Nano-Structured Composite Layers Synthesized by Electrochemical Method**, IOP Conf. Ser.: Mater. Sci. Eng. 572 (2019) 012004, <https://iopscience.iop.org/article/10.1088/1757-899X/572/1/012004/pdf>
DOI: 10.1088/1757-899X/572/1/012004

3) L Dragus, L Benea, **N Simionescu**, A Ravoiiu, V Neaga, **Effect of the Inflammatory Conditions and Albumin Presence on the Corrosion Behavior of Grade 5 Titanium Alloy in Saliva Biological Solution**, IOP Conf. Ser.: Mater. Sci. Eng. 572 (2019) 012005. <https://iopscience.iop.org/article/10.1088/1757-899X/572/1/012005/pdf>
DOI: 10.1088/1757-899X/572/1/012005.

4) Anca Ravoiiu, **Nicoleta Simionescu**, Lidia Benea, **Influence of different concentration of hydrogen peroxide on the corrosion behavior of Ti-6Al-4V alloy immersed in physiological solution**, IOP Conf. Ser.: Mater. Sci. Eng. 572 (2019) 012006. <https://iopscience.iop.org/article/10.1088/1757-899X/572/1/012006/pdf>
DOI: 10.1088/1757-899X/572/1/012006.

5) **N Simionescu**, L Benea and V M Dumitrascu, **The Synergistic Effect of Proteins and Reactive Oxygen Species on Electrochemical Behaviour of 316L Stainless Steel for Biomedical Applications**. IOP Conf. Series: Materials Science and Engineering 374 (2018) 012058. <https://iopscience.iop.org/article/10.1088/1757-899X/374/1/012058/pdf>
Accession Number: WOS:000446775900058
doi: 10.1088/1757-899X/374/1/012058

6) V M Dumitrascu, L Benea and **N L Simionescu**, **Evaluation of Sealing Process on the Surface Properties of Nanoporous Aluminum Oxide Layers Electrochemically Growth on 1050 Aluminum Alloy Surface**. IOP Conf. Series: Materials Science and Engineering 374 (2018) 012013. <https://iopscience.iop.org/article/10.1088/1757-899X/374/1/012013/pdf>
Accession Number: WOS:000446775900013
doi:10.1088/1757-899X/374/1/012013.

8.2.3. Publications in journals indexed in international databases - 5

1) Lidia Benea, **Nicoleta Simionescu**, **Effect of Biological Solution and pH on Corrosion Resistance of 304L SS for Dental Brackets**, *Revista de Chimie*, 2020, Vol. 71, Issue 4, p. 180-187, <https://doi.org/10.37358/RC.20.4.8056>.

2) L Benea , **N Simionescu**, **Evaluation of corrosion resistance of implant-use Ti6Al4V alloy in Hank biological solution in the presence of microorganism's metabolic product Lactic Acid**, *The Annals of "Dunarea de Jos" University of Galati Fascicle IX. Metallurgy and Materials Science*, No.



1 - 2020, ISSN 2668-4748; e-ISSN 2668-4756, Pages 31-38. <https://doi.org/10.35219/mms.2020.1.04>.

3) **Nicoleta Simionescu**, Lidia Benea, Anca RavoIU, **Effect of hydrogen peroxide addition to phosphate buffered saline solutions on corrosion resistance of 316L stainless steel**, *Proceeding Volume of 18th International Multidisciplinary Scientific GeoConference SGEM 2018*, Volume:18, Book number: 6.1, Pages:169-176, ISSN: 1314-2704, 24. Section Micro and Nano Technologies, 30 June - 9 July, 2018, Albena, Bulgaria.

Doi: 10.5593/sgem2018/6.1.

4) Valentin Marian Dumitrascu, Lidia Benea, **Nicoleta Lucica Simionescu**, **Surfaces morphology, roughness and wetting properties of nanoporous aluminum oxide film formed on 1050 aluminum alloy by controlled electrochemical oxidation**, *Proceeding Volume of 18th International Multidisciplinary Scientific GeoConference SGEM 2018*, Volume:18, Book number: 6.1, Pages:473-480, ISSN: 1314-2704, 24. Section Micro and Nano Technologies, 30 June - 9 July, 2018, Albena, Bulgaria.

Doi: 10.5593/sgem2018/6.1.

5) **Nicoleta Lucica Simionescu**, Lidia Benea; **The corrosion behavior of 316L stainless steel in different simulated body fluids solutions**, *Proceeding Volume of 17th International Multidisciplinary Scientific GeoConference SGEM 2017*, Volume:17, Book number: 61, Pages: 353-360, ISSN: 1314-2704, 24. Section Micro and Nano Technologies, 29 June - 5 July, 2017, Albena, Bulgaria.

<https://doi.org/10.5593/sgem2017/61>

8.2.4. Papers and posters presented at international congresses, workshops and seminars - 16

1) **N Simionescu**, L Benea, A Chiriac, The Effect of H₂O₂ and Lactic Acid addition in Biological Saliva on the Corrosion Behaviour of 304L Stainless Steel, *Poster presentation*. International Conference on Innovative Research, Iasi, 21th – 22th of May 2020.

http://www.euroinvent.org/conference/doc/Program_ICIR_2020.pdf

2) **N Simionescu**, L Benea, J P Celis, **Wear-Corrosion Response of Cerium Oxide Reinforced Cobalt Hybrid Composite Layers in Biological Solution**, *Oral presentation*. International Conference on Innovative Research, Iasi, 16th – 17th of May 2019.

http://www.euroinvent.org/conference/doc/Program_ICIR2019.pdf

3) **Nicoleta Simionescu**, Lidia Benea, Anca RavoIU, **The influence of dispersed CeO₂ nanoparticles on the electro-crystallization mechanism of cobalt**, *Oral presentation*. The Vth international conference "New trends in environmental and materials engineering" (TEME 2019), 23-25 October 2019, Galați, Romania.

www.teme.ugal.ro

http://www.teme.ugal.ro/Program_COMPLET_TEME_2019.pdf

4) Anca RavoIU, Lidia Benea, **Nicoleta Lucica Simionescu**, Alexandru Chiriac, **Influence of inflammatory conditions on the corrosion behavior of titanium alloy in buffered biological solution**, *Oral presentation*. The Vth international conference "New trends in environmental and materials engineering" (TEME 2019), 23-25 October 2019, Galați, Romania.

www.teme.ugal.ro

http://www.teme.ugal.ro/Program_COMPLET_TEME_2019.pdf

5) L Benea , **N Simionescu**, **Corrosion Behavior of Ni/WC Nano-Structured Composite Layers Synthesized by Electrochemical Method**, *Oral presentation*. International Conference on Innovative Research, Iasi, 16th – 17th of May 2019. **This work received the BEST ORAL**



PRESENTATION award.

http://www.euroinvent.org/conference/doc/Program_ICIR2019.pdf

6) L Dragus, L Benea, **N Simionescu**, A RavoIU, V Neaga, **Effect of the Inflammatory Conditions and Albumin Presence on the Corrosion Behavior of Grade 5 Titanium Alloy in Saliva Biological Solution**, *Oral presentation*. International Conference on Innovative Research, Iasi, 16th – 17th of May 2019

http://www.euroinvent.org/conference/doc/Program_ICIR2019.pdf

7) Anca RavoIU, **Nicoleta Simionescu**, Lidia Benea, **Influence of different concentration of hydrogen peroxide on the corrosion behavior of Ti-6Al-4V alloy immersed in physiological solution**, *Oral presentation*. International Conference on Innovative Research, Iasi, 16th – 17th of May 2019

http://www.euroinvent.org/conference/doc/Program_ICIR2019.pdf

8) **Nicoleta Simionescu**, Lidia Benea, Anca RavoIU, **Effect of hydrogen peroxide addition to phosphate buffered saline solutions on corrosion resistance of 316L stainless steel**, *Oral presentation*. 18th International Multidisciplinary Scientific GeoConference SGEM 2018, 24. Section Micro and Nano Technologies, 30 June - 9 July, 2018, Albena, Bulgaria.

www.sgem.org

<http://www.sgem.org/index.php/sgem-deadline/sgem-programme2018>.

9) Valentin Marian Dumitrascu, Lidia Benea, **Nicoleta Lucica Simionescu**, **Surfaces morphology, roughness and wetting properties of nanoporous aluminum oxide film formed on 1050 aluminum alloy by controlled electrochemical oxidation**. *Oral presentation*. 18th International Multidisciplinary Scientific GeoConference SGEM 2018, 24. Section Micro and Nano Technologies, 30 June - 9 July, 2018, Albena, Bulgaria, www.sgem.org

<http://www.sgem.org/index.php/sgem-deadline/sgem-programme2018>.

10) **N Simionescu**, L Benea and V M Dumitrascu, **The Synergistic Effect of Proteins and Reactive Oxygen Species on Electrochemical Behaviour of 316L Stainless Steel for Biomedical Applications**. *Poster presentation*. ICIR Euroinvent 2018, International Conference on Innovative Research, Iasi, 17th – 18th of May 2018.

http://www.euroinvent.org/conference/doc/Program_ICIR2018.pdf

11) V M Dumitrascu, L Benea and **N L Simionescu**. **Evaluation of Sealing Process on the Surface Properties of Nanoporous Aluminum Oxide Layers Electrochemically Growth on 1050 Aluminum Alloy Surface**. *Oral presentation*. ICIR Euroinvent 2018, International Conference on Innovative Research, Iasi, 17th – 18th of May 2018.

http://www.euroinvent.org/conference/doc/Program_ICIR2018.pdf

12) **Nicoleta Simionescu**, Lidia Benea, Anca RavoIU, **The effect of commercial juices on the corrosion resistance of 316L stainless steel used for orthodontic applications**. *Oral presentation*. UgalMat 2018 - Conference on Material Science & Engineering, October 11-13, 2018, Galati, Romania.

www.ugalmat.ugal.ro/

<http://www.ugalmat.ugal.ro/FINAL%20PROGRAMME%20UgalMat2018.pdf>

13) **Nicoleta Simionescu**, Sara Hondrilă, Lidia Benea, **Corrosion - A major problem in the functioning of the installations: Assessment of copper and brass corrosion resistance in water and chloride content solutions**. *Oral presentation*. UgalMat 2018 - Conference on Material science & engineering, October 11-13, 2018, Galati, Romania.

www.ugalmat.ugal.ro/

<http://www.ugalmat.ugal.ro/FINAL%20PROGRAMME%20UgalMat2018.pdf>



14) Lidia Benea, **Nicoleta Simionescu**, Anca Ravoii, **Corrosion resistance of 304L stainless steel for orthodontic fixed appliances in saliva and different pH solutions from food or drinks.** *Oral presentation.* UgalMat 2018 - Conference on Material Science & Engineering, October 11-13, 2018, Galati, Romania.

www.ugalmat.ugal.ro/

<http://www.ugalmat.ugal.ro/FINAL%20PROGRAMME%20UgalMat2018.pdf>

15) Valentin Dumitrascu, **Nicoleta Simionescu**, Lidia Benea, **Optimizing the electrochemical parameters to obtain a nanoporous aluminum oxide on 1050 aluminum alloy: A SEM-EDX and hydrophobicity study.** *Oral presentation.* UgalMat 2018 - Conference on Material Science & Engineering, October 11-13, 2018, Galati, Romania.

www.ugalmat.ugal.ro/

<http://www.ugalmat.ugal.ro/FINAL%20PROGRAMME%20UgalMat2018.pdf>

16) **Nicoleta Simionescu**, Lidia Benea. **Electrochemical in-vitro properties of 316L stainless steel for orthodontic applications,** *Oral presentation.* The fourth international conference "New trends in environmental and materials engineering" (TEME 2017), 25-27 October 2017, Galați, Romania.

www.teme.ugal.ro

http://www.teme.ugal.ro/Program_TEME_2017.pdf

8.2.5. Papers and posters presented at national congresses - 12

1) **Nicoleta Simionescu**, Lidia Benea, **Influence of current density on the electrodeposition of CeO₂ nanoparticle into cobalt matrix on 304L stainless steel substrate.**

Oral presentation. SCIENTIFIC CONFERENCE OF DOCTORAL SCHOOLS, SCDS-UDJG 2020, The 8th Edition, Perspectives and challenges in doctoral research, GALAȚI, 18th-19th of June 2020. S.6: Future of Eco-nanotechnologies, Functional Materials and Coatings.

<http://www.cssd-udjg.ugal.ro/>

<http://www.cssd-udjg.ugal.ro/index.php/programme-2020>

2) Lidia Benea, **Nicoleta Simionescu**, **The influence of different concentration of Lactic acid added in simulated body fluid solution as a function in time on the corrosion behavior of titanium alloy.**

Oral presentation. SCIENTIFIC CONFERENCE OF DOCTORAL SCHOOLS, SCDS-UDJG 2020, The 8th Edition, Perspectives and challenges in doctoral research, GALAȚI, 18th-19th of June 2020. S.6: Future of Eco-nanotechnologies, Functional Materials and Coatings.

<http://www.cssd-udjg.ugal.ro/>

<http://www.cssd-udjg.ugal.ro/index.php/programme-2020>

3) **Nicoleta Lucica Simionescu**, Valentin Marian Dumitrascu, Lidia Benea, **Improving corrosion resistance of aluminium alloy by top-down nano-electrochemical film growth.**

Poster presentation. SCIENTIFIC CONFERENCE OF DOCTORAL SCHOOLS, SCDS-UDJG 2020, The 8th Edition, Perspectives and challenges in doctoral research, GALAȚI, 18th-19th of June 2020. S.6: Future of Eco-nanotechnologies, Functional Materials and Coatings.

<http://www.cssd-udjg.ugal.ro/>

<http://www.cssd-udjg.ugal.ro/index.php/programme-2020>

4) **Nicoleta Lucica Simionescu**, Laurentiu Mardare, Lidia Benea, **Modification of surface properties as roughness, microhardness and hydrophobicity of polymeric primer used to protect maritime structures made of E32 steel.**

Poster presentation. SCIENTIFIC CONFERENCE OF DOCTORAL SCHOOLS, SCDS-UDJG 2020, The 8th Edition, Perspectives and challenges in doctoral research, GALAȚI, 18th-19th of June 2020. S.6: Future of Eco-nanotechnologies, Functional Materials and Coatings.

<http://www.cssd-udjg.ugal.ro/>



<http://www.cssd-udjg.ugal.ro/index.php/programme-2020>

5) **Nicoleta Simionescu**, Lidia Benea, **Tribocorrosion behavior of 304L stainless steel in sliding contact immersed in Hank biological solution.**

Oral presentation. SCIENTIFIC CONFERENCE OF DOCTORAL SCHOOLS, SCDS-UDJG 2019, The seventh Edition, Perspectives and challenges in doctoral research, GALAȚI, 13th-14th of June 2019. S.5.1: Emerging nanotechnology and future of advanced materials and coatings.

<http://www.cssd-udjg.ugal.ro/>

http://www.cssd-udjg.ugal.ro/files/2019/Program_detaliat_al_conferintei_nou_2.pdf

6) **Nicoleta Simionescu**, Lidia Benea. **Surface modification of metallic biomaterials to improve the body integration and corrosion resistance in body environment.**

Oral presentation. SCIENTIFIC CONFERENCE OF DOCTORAL SCHOOLS, SCDS-UDJG 2019, The seventh Edition, Perspectives and challenges in doctoral research, GALAȚI, 13th-14th of June 2019. S.5.1: Emerging nanotechnology and future of advanced materials and coatings. **This work received the first prize.**

<http://www.cssd-udjg.ugal.ro/>

http://www.cssd-udjg.ugal.ro/files/2019/Program_detaliat_al_conferintei_nou_2.pdf

7) Lidia Benea, **Nicoleta Simionescu**, Laurențiu Dragus, Veaceslav Neaga, Anca Ravoii. **Effect of the presence of hydrogen peroxide reactive oxygen specie on the corrosion behavior of titanium alloy in buffered saline solution.**

Oral presentation. SCIENTIFIC CONFERENCE OF DOCTORAL SCHOOLS, SCDS-UDJG 2019, The seventh Edition, Perspectives and challenges in doctoral research, GALAȚI, 13th-14th of June 2019. S.5.1: Emerging nanotechnology and future of advanced materials and coatings.

<http://www.cssd-udjg.ugal.ro/>

http://www.cssd-udjg.ugal.ro/files/2019/Program_detaliat_al_conferintei_nou_2.pdf

8) **Nicoleta SIMIONESCU**, Lidia Benea, Anca Ravoii. **Effect of human serum albumin on the corrosion behaviour of 316L stainless steel in phosphate buffered saline solution.**

Oral presentation. SCIENTIFIC CONFERENCE OF DOCTORAL SCHOOLS, SCDS-UDJG 2018, The Sixth Edition, Perspectives and challenges in doctoral research, GALAȚI, 7th-8th of June 2018. S.5.1: Emerging nanotechnology and future of advanced materials and coatings. **This work received the third prize.**

<http://www.cssd-udjg.ugal.ro/>

http://www.cssd-udjg.ugal.ro/files/2018/05_Program_detaliat_al_conferintei_2018.pdf

9) Lidia Benea, **Nicoleta Simionescu**, Anca Ravoii. **Effect of pH and biological solution composition on corrosion resistance of 304L stainless steel for orthodontic fixed appliances.**

Oral presentation. SCIENTIFIC CONFERENCE OF DOCTORAL SCHOOLS, SCDS-UDJG 2018, The Sixth Edition, Perspectives and challenges in doctoral research, GALAȚI, 7th-8th of June 2018. S.5.1: Emerging nanotechnology and future of advanced materials and coatings.

<http://www.cssd-udjg.ugal.ro/>

http://www.cssd-udjg.ugal.ro/files/2018/05_Program_detaliat_al_conferintei_2018.pdf

10) Anca Răvoiu, Lidia Benea, **Nicoleta Simionescu**, Alexandru Chiriac. **Hydrogen peroxide and its effect on electrochemical behavior of titanium implant alloy.**

Oral presentation. SCIENTIFIC CONFERENCE OF DOCTORAL SCHOOLS, SCDS-UDJG 2018, The Sixth Edition, Perspectives and challenges in doctoral research, GALAȚI, 7th-8th of June 2018. S.5.1: Emerging nanotechnology and future of advanced materials and coatings.

<http://www.cssd-udjg.ugal.ro/>

http://www.cssd-udjg.ugal.ro/files/2018/05_Program_detaliat_al_conferintei_2018.pdf

11) Valentin Marian Dumitrașcu, Lidia Benea, **Nicoleta Lucica Simionescu**. **Performance evaluation of nanoporous aluminum oxide layers obtained by controlled anodic oxidation**



process.

Oral presentation. SCIENTIFIC CONFERENCE OF DOCTORAL SCHOOLS, SCDS-UDJG 2018, The Sixth Edition, Perspectives and challenges in doctoral research, GALAȚI, 7th-8th of June 2018. S.5.1: Emerging nanotechnology and future of advanced materials and coatings.

<http://www.cssd-udjg.ugal.ro/> **This work received the first prize.**

http://www.cssd-udjg.ugal.ro/files/2018/05_Program_detaliat_al_conferintei_2018.pdf

12) **Nicoleta Simionescu**, Lidia Benea, **Electrochemical Study of 316L Stainless Steel as an Effective Biomaterial for Orthodontic Applications**, *Oral presentation.* SCIENTIFIC CONFERENCE OF DOCTORAL SCHOOLS, SCDS-UDJG 2017, The fifth Edition, Perspectives and challenges in doctoral research, GALAȚI, 8th-9th of June 2017. S.4: Advanced investigation methods in environment and biohealth. **This work received the third prize.**

<http://www.cssd-udjg.ugal.ro/>

http://www.cssd-udjg.ugal.ro/files/2017/Program_detaliat_al_conferintei_2017_FINAL.pdf

8.2.6 Research results awards from the executive unit for financing higher education, research, development and innovations

1) L Benea, L Mardare, **Nicoleta Simionescu**, **Anticorrosion performances of modified polymeric coatings on E32 naval steel in sea water**, *Progress in Organic Coatings* 123 (2018) 120 - 127, <https://doi.org/10.1016/j.porgcoat.2018.06.020>, Q1, I.F. = 3.420. WOS:000444357000013. Nr. curent 94, Lista 10.

[https://uefiscdi.gov.ro/resource-](https://uefiscdi.gov.ro/resource-80293?&wtok=&wtkps=XY1RDsIgEETvwrfFLpSWbu9gTDxBBawYLVhaMTheXeiP0a+d7Myb6b)

80293?&wtok=&wtkps=XY1RDsIgEETvwrfFLpSWbu9gTDxBBawYLVhaMTheXeiP0a+d7Myb6bHGV0COJFhNuoAVQwKVF7MQ/n52se7BjpVfymMt26GAZpAXxQsIz3aKIROAxOabQAFZpDK1k2URqjYHGIRa+3F/2PKmZJLJUsvSOj3s2EAggNw4GutWKNdHwMlkt9g2o1m3U3q5vRyNdRNA13MyQalLX1YE2k/zVa5K+neHw==&wchk=b330d4c966bfffdeca666071794baf014e053347

8.2.7 ISI Quotations (Clarivate Analytics) - 7

1. L Dragus, L Benea, **N Simionescu**, A Ravoiiu, V Neaga, **Effect of the Inflammatory Conditions and Albumin Presence on the Corrosion Behavior of Grade 5 Titanium Alloy in Saliva Biological Solution**, *IOP Conf. Ser.: Mater. Sci. Eng.* 572 (2019) 012005. <https://iopscience.iop.org/article/10.1088/1757-899X/572/1/012005/pdf>

DOI: 10.1088/1757-899X/572/1/012005.

Quoted 1 time in ISI listed journal

1.1. Hedberg, Y. S., Gamna, F., Padoan, G., Ferraris, S., Cazzola, M., Herting, G., Odnevall Wallinder, I. (2020). Surface modified Ti6Al4V for enhanced bone bonding ability – Effects of silver and corrosivity at simulated physiological conditions from a corrosion and metal release perspective. *Corrosion Science*, 108566. doi:10.1016/j.corsci.2020.108566

2. **N Simionescu**, L Benea and V M Dumitrascu, **The Synergistic Effect of Proteins and Reactive Oxygen Species on Electrochemical Behaviour of 316L Stainless Steel for Biomedical Applications**. *IOP Conf. Series: Materials Science and Engineering* 374 (2018) 012058. <https://iopscience.iop.org/article/10.1088/1757-899X/374/1/012058/pdf>

Accession Number: WOS:000446775900058

doi:10.1088/1757-899X/374/1/012058.

Quoted 1 time in bachelor's thesis

2.1. López Puerto, M.J. (2019). Progresos en el desarrollo de soportes metálicos para su empleo en prótesis e implantes. (Trabajo Fin de Grado Inédito, Grado en Farmacia). Universidad de Sevilla, Sevilla, Departamento de Química Física.



3. Lidia Benea, Laurentiu Mardare, **Nicoleta Simionescu**, **Anticorrosion performances of modified polymeric coatings on E32 naval steel in sea water**, *Progress in Organic Coatings*, **2018**, vol 123, p. 120-127. Impact Factor = 3.420, **Q1**, <https://doi.org/10.1016/j.porgcoat.2018.06.020>

Accession Number: WOS:000444357000013

Quoted 6 time in ISI listed journal

3.1. Foteinidis G, Tsirka K, Tzounis L, Baltzis D, Paipetis A.S. The Role of Synergies of MWCNTs and Carbon Black in the Enhancement of the Electrical and Mechanical Response of Modified Epoxy Resins. 2019, *Applied Sciences*, 9(18), 3757. doi:10.3390/app9183757.

3.2. Radhamani A, Lau H.C, Ramakrishna S. Nanocomposite coatings on steel for enhancing the corrosion resistance: A review. 2019, *Journal of Composite Materials*, 002199831985780. doi:10.1177/0021998319857807.

3.3. Solano, R., Patiño-Ruiz, D., & Herrera, A. (2020). Preparation of modified paints with nanostructured additives and its potential applications. *Nanomaterials and Nanotechnology*, 10, 184798042090918. doi:10.1177/1847980420909188.

3.4. Chen, L., Yu, Z., Yin, D., & Cao, K. (2020). Preparation and anticorrosion properties of BTA@HNTs-GO nanocomposite smart coatings. *Composite Interfaces*, 1–16. doi:10.1080/09276440.2020.1733371

3.5. Ma, Z., Sun, M., Li, A., Zhu, G., & Zhang, Y. (2020). Anticorrosion behavior of polyvinyl butyral (PVB) / polymethylhydrosiloxane (PMHS) / chitosan (Ch) environment-friendly assembled coatings. *Progress in Organic Coatings*, 144, 105662. doi:10.1016/j.porgcoat.2020.105662

3.6. Manoj, M., Kumaravel, A., Mangalam, R. et al. Exploration of high corrosion resistance property of less hazardous pyrazolidine-based benzoxazines in comparison with bisphenol-F derivatives. *J Coat Technol Res* (2020). <https://doi.org/10.1007/s11998-019-00312-4>.



REFERENCES

- [1] Zavaglia C.A.C., Prado da Silva M.H., Feature Article: Biomaterials, Reference Module in Materials Science and Materials Engineering (2016) 1-5. doi:10.1016/B978-0-12-803581-8.04109-6
- [4] Donglu S., Introduction to Biomaterials, Tsinghua University Press, 2006, ISBN 981-256-627-9, China. <http://samme.parsaspace.com/Introduction%20to%20Biomaterials%20%20Donglu%20Shi.pdf>
- [5] Biomaterials, edited by Joyce. Y. Yong, Joseph. D. Bronzino, 2007, CRC Press Taylor and Francis Group, ISBN-13: 978-0-8493-7888-1, London.
- [6] Williams, D.F., 1999. The Williams Dictionary of Biomaterials. Liverpool: Liverpool University Press. (Print). <https://doi.org/10.5949/UPO9781846314438>.
- [7] Noam E., Corrosion of metallic biomaterials: A Review, Materials, 2019, 12 (3), 407; doi:10.3390/ma12030407
- [8] Bauer, S., Schmuki, P., von der Mark, K., & Park, J. (2013). Engineering biocompatible implant surfaces. Progress in Materials Science, 58(3), 261–326. doi:10.1016/j.pmatsci.2012.09.001
- [9] Patitapabana P., Ajit B., Subash C.M., Classification of Biomaterials used in Medicine, International Journal of Advances in Applied Sciences (IJAAS), Vol.1, No.3, Month 2012, pp. 31-35.
- [10] Mabileau, G., Kwon, Y.-M., Pandit, H., Murray, D. W., & Sabokbar, A. (2008). Metal-on-metal hip resurfacing arthroplasty: A review of periprosthetic biological reactions. Acta Orthopaedica, 79(6), 734–747. doi:10.1080/17453670810016795
- [11] Pibul I., Biomaterials an Overview, Journal of Metals, Materials and Minerals, vol 11, nr.1, 2001, 15-21.
- [26] Miran Mozetic Surface Modification to Improve Properties of Materials, Materials 2019, 12, 441; doi:10.3390/ma12030441
- [27] Santiago Arango , Alejandro Peláez-Vargas and Claudia García, Coating and Surface Treatments on Orthodontic Metallic Materials, Coatings 2013, 3, 1-15; doi:10.3390/coatings3010001
- [28] Shaurya Prakash, M.B. Karacor , S. Banerjee, Surface modification in microsystems and nanosystems, Surface Science Reports 64 (2009) 233–254. doi:10.1016/j.surfrep.2009.05.001
- [51] Gamburg, Y. D., Zangari, G. (2011). Theory and Practice of Metal Electrodeposition. doi:10.1007/978-1-4419-9669-5
- [52] Nasirpouri, F. (2017). Electrodeposition of Nanostructured Materials. Springer Series in Surface Sciences. doi:10.1007/978-3-319-44920-3
- [53] Gurrappa, I., & Binder, L. (2008). Electrodeposition of nanostructured coatings and their characterization—A review. Science and Technology of Advanced Materials, 9(4), 043001. doi:10.1088/1468-6996/9/4/043001
- [62]. Benea, L., Dănilă, E. (2016). Electrochemical Codeposition of UHMWPE Biopolymer into Cobalt Matrix for Biomedical Applications. Key Engineering Materials, 699, 57–62. doi:10.4028/www.scientific.net/kem.699.
- [63]. L. Benea, M. Mardare-Prlea, Electrodeposition of UHMWPE particles with cobalt for biomedical applications, Digest Journal of Nanomaterials and Biostructures Vol. 6, No 3, July-September 2011, p. 1025-1034.
- [66]. Benea, L., Ponthiaux, P., Wenger, F. (2011). Co-ZrO₂ electrodeposited composite coatings exhibiting improved micro hardness and corrosion behavior in simulating body fluid solution. Surface and Coatings Technology, 205(23-24), 5379–5386. doi:10.1016/j.surfcoat.2011.05.050
- [67]. Nicholus Malatji and Patricia A.I. Popoola. (2015) Tribological and Corrosion Performance of Electrodeposited Nickel Composite Coatings, Electrodeposition of Composite Materials, <http://dx.doi.org/10.5772/62170>.
- [68]. Walsh, F. C., Ponce de Leon, C. (2014). A review of the electrodeposition of metal matrix composite coatings by inclusion of particles in a metal layer: an established and diversifying technology. Transactions of the IMF, 92(2), 83–98. doi:10.1179/0020296713z.000000000161

- [69]. Güler, E. S. (2016). Effects of Electroplating Characteristics on the Coating Properties. Electrodeposition of Composite Materials. doi:10.5772/61745
- [70]. Guglielmi, N. (1972). Kinetics of the Deposition of Inert Particles from Electrolytic Baths J. Electrochem. Soc., 119, 1009–1012. doi:10.1149/1.2404383.
- [76] Singh VB, Singh DK (2014) An Overview on the Preparation, Characterization and Properties of Electrodeposited-Metal, Matrix Nanocomposites. *Nanosci Technol* 1(3): 1-20. DOI: <http://dx.doi.org/10.15226/2374-8141/1/3/00120>
- [77] Abdel-Karim, R. (2016). Electrochemical Synthesis of Nanocomposites. Electrodeposition of Composite Materials. doi:10.5772/62189
- [78] Casati, R., Vedani, M. (2014). Metal Matrix Composites Reinforced by Nano-Particles—A Review. *Metals*, 4(1), 65–83. doi:10.3390/met4010065
- [79] Mahdavi, S., Allahkaram, S. R. (2015). Composition, characteristics and tribological behavior of Cr, Co–Cr and Co–Cr/TiO₂ nano-composite coatings electrodeposited from trivalent chromium based baths. *Journal of Alloys and Compounds*, 635, 150–157. doi:10.1016/j.jallcom.2015.02.119
- [81] Gomes A, Pereira I, B. Fernandez, R. Pereiro, *Advances in Nanocomposites - Synthesis, Characterization and Industrial Applications*, (edit. B. S. R. Reddy) chapter 21, Electrodeposition of Metal Matrix Nanocomposites: Improvement of the Chemical Characterization Techniques, INTECH, 2011. <https://www.intechopen.com/books/electrodeposition-of-composite-materials/electrochemical-synthesis-of-nanocomposites>
- [88] Germain, M. A., Hatton, A., Williams, S., Matthews, J. B., Stone, M. H., Fisher, J., Ingham, E. (2003). Comparison of the cytotoxicity of clinically relevant cobalt–chromium and alumina ceramic wear particles in vitro. *Biomaterials*, 24(3), 469–479. doi:10.1016/s0142-9612(02)00360-5
- [89] Willert, H.-G., Buchhorn, G. H., Fayyazi, A., Flury, R., Windler, M., Köster, G., Lohmann, C. H. (2005). Metal-on-Metal Bearings and Hypersensitivity in Patients with Artificial Hip Joints. *The Journal of Bone & Joint Surgery*, 87(1), 28–36. doi:10.2106/jbjs.a.02039pp
- [90] N. Hallab, K. Merritt and J. Jacobs, Metal Sensitivity in Patients with Orthopaedic Implants, *J. Bone Joint Surg. Am.*, 2001, 83(3), 428–428. DOI: 10.2106/00004623-200103000-00017
- [91] Abdeen, D., El Hachach, M., Koc, M., Atieh, M. (2019). A Review on the Corrosion Behaviour of Nanocoatings on Metallic Substrates. *Materials*, 12(2), 210. doi:10.3390/ma12020210
- [92] Rezende, T. G. L., Cesar, D. V., do Lago, D. C. B., Senna, L. F. (2016). A review of Corrosion Resistance Nanocomposite Coatings. Electrodeposition of Composite Materials. doi:10.5772/62048
- [102] Mathew, M. T., Srinivasa Pai, P., Pourzal, R., Fischer, A., & Wimmer, M. A. (2009). Significance of Tribocorrosion in Biomedical Applications: Overview and Current Status. *Advances in Tribology*, 2009, 1–12. doi:10.1155/2009/250986
- [103] Celis, Jean-Pierre, Ponthiaux, P. (2012). Testing tribocorrosion of passivating materials supporting research and industrial innovation: Testing Tribocorrosion of Passivating Materials Supporting Research and Industrial Innovation: Handbook. 1-13. European Federation of Corrosion, nr. 62, ISBN-13: 9781907975202.
- [110] Diomidis, N., Celis, J.-P., Ponthiaux, P., Wenger, F. (2009). A methodology for the assessment of the tribocorrosion of passivating metallic materials. *Lubrication Science*, 21(2), 53–67. doi:10.1002/lis.73
- [114] Wood, R. J. K. (2007). Tribo-corrosion of coatings: a review. *Journal of Physics D: Applied Physics*, 40(18), 5502–5521. doi:10.1088/0022-3727/40/18/s10
- [115] Sorcaru F. S, Teza de doctorat, Suprafețe funcționale Co/nano-ZrO₂ obținute prin electrodepunere pentru utilizarea în industrie și biomedicină, Galati, 2012. Universitatea Dunarea de Jos din Galati.
- [119] Sajad Hussain Din, M. A. Shah , N. A. Sheikh , M. Mursaleen Butt, Nano-composites and their applications: A review, EnPress Publisher, LLC. United States, 2018, DOI: 10.24294/can.v0i0.875.
- [121] Subramanian, S. B., Francis, A. P., Devasena, T. (2014). Chitosan–starch nanocomposite particles as a drug carrier for the delivery of bis-desmethoxy curcumin analog. *Carbohydrate Polymers*, 114, 170–178. doi:10.1016/j.carbpol.2014.07.053
- [122] Wang, B.-L., Liu, X.-S., Ji, Y., Ren, K.-F., Ji, J. (2012). Fast and long-acting antibacterial properties of chitosan-Ag/polyvinylpyrrolidone nanocomposite films. *Carbohydrate Polymers*, 90(1), 8–15. doi:10.1016/j.carbpol.2012.03.080
- [123] Nathanael, A. J., Lee, J. H., Mangalaraj, D., Hong, S. I., Rhee, Y. H. (2012). Multifunctional

- properties of hydroxyapatite/titania bio-nano-composites: bioactivity and antimicrobial studies. *Powder Technology*, 228, 410–415. doi:10.1016/j.powtec.2012.06.001
- [124] Khalid, A., Khan, R., Ul-Islam, M., Khan, T., Wahid, F. (2017). Bacterial cellulose-zinc oxide nanocomposites as a novel dressing system for burn wounds. *Carbohydrate Polymers*, 164, 214–221. doi:10.1016/j.carbpol.2017.01.061
- [125] Baghayeri, M., Nazarzadeh Zare, E., Mansour Lakouraj, M. (2014). A simple hydrogen peroxide biosensor based on a novel electro-magnetic poly(p-phenylenediamine)@Fe₃O₄ nanocomposite. *Biosensors and Bioelectronics*, 55, 259–265. doi:10.1016/j.bios.2013.12.033
- [126] Hasnain, M. S., Nayak, A. K. (2019). Nanocomposites for improved orthopedic and bone tissue engineering applications. *Applications of Nanocomposite Materials in Orthopedics*, 145–177. doi:10.1016/b978-0-12-813740-6.00008-9
- [138] Felicia Bratu, Lidia Benea, Jean-Pierre Celis, The influence of fretting parameters on tribocorrosion behaviour of AISI 304L stainless steel in ringer solution, *Rev. Chim. (Bucuresti)*, 59 Nr. 3, 2008, 346-350. <https://doi.org/10.37358/RC.08.3.1760>
- [212] Zhang, G., Xu, B., Chong, H., Wei, W., Wang, C., Wang, G. (2019). Effect of glyphosate on X-ray diffraction of copper films prepared by electrochemical deposition. *RSC Advances*, 9(25), 14016–14023. doi:10.1039/c9ra01385g
- [228]. Vetter, K. J. (1967). Methods of Determining Electrochemical Reaction Mechanisms. *Electrochemical Kinetics*, 396–454. doi:10.1016/b978-1-4832-2936-2.50007-x
- [229]. Benea, L. *Electrodepuneri composite in teorie si practicea*, Editura Porto Franco, Galati, 1998, ISBN: 973-557-490-X.
- [232]. Benea, L., Danaila, E. (2016). Nucleation and Growth Mechanism of Ni/TiO₂ Nanoparticles Electro-Codeposition. *Journal of The Electrochemical Society*, 163(13), D655–D662. doi:10.1149/2.0591613jes
- [233]. Benea, L., Bonora, P. L., Borello, A., Martelli, S., Wenger, F., Ponthiaux, P., Galland, J. (2001). Composite Electrodeposition to Obtain Nanostructured Coatings. *Journal of The Electrochemical Society*, 148(7), C461. doi:10.1149/1.1377279
- [234]. Cesiulis, H., Tsyntaru, N., Ramanavicius, A., Ragoisha, G. (2016). The Study of Thin Films by Electrochemical Impedance Spectroscopy. *NanoScience and Technology*, 3–42. doi:10.1007/978-3-319-30198-3_1
- [239]. I. Danaee. (2013). Theoretical and experimental studies of layer by layer nucleation and growth of palladium on stainless steel, *Chemija*. 24 (2), 128–136. <http://mokslozurnalai.lmaleidykla.lt/publ/0235-7216/2013/2/128-136.pdf>
- [241]. K, Sunil., S, Pande., P, Verma. (2015). Factor Effecting Electro-Deposition Process. *International Journal of Current Engineering and Technology*, 5(2), 700-703. <https://inpressco.com/wp-content/uploads/2015/03/Paper18700-703.pdf>
- [242]. S, Fazli., Bahrololoom, M. E. (2016). Effect of plating time on electrodeposition of thick nanocrystalline permalloy foils. *Transactions of the IMF*, 94(2), 92–98. doi:10.1080/00202967.2015.1122918
- [243]. D, Oloruntoba., O, Eghwubare., O, Oluwole. (2011). Effect of Some Process Variables on Nickel Electroplating of Low Carbon Steel, *Leonardo El J Pract Technol*, 1-12. http://lejpt.academicdirect.org/A18/get_htm.php?htm=079_094
- [244]. Pavlov I. A, Teza de doctorat, *Influența tratamentelor electrochimice a suprafețelor (straturi nanocompozite în matrice de nichel) asupra rezistenței la coroziune și uzură*, Galati, 2012. Universitatea Dunarea de Jos din Galati.
- [245]. Benea, L., Celis, J.-P. (2016). Effect of Nano-TiC Dispersed Particles and Electro-Codeposition Parameters on Morphology and Structure of Hybrid Ni/TiC Nanocomposite Layers. *Materials*, 9(4), 269. doi:10.3390/ma9040269
- [247]. Kuo, S. (2004). The influence of process parameters on the MoS₂ content of Ni-MoS₂ composite coating by the robust design method. *Journal of the Chinese Institute of Engineers*, 27(2), 243–251. doi:10.1080/02533839.2004.9670869.
- [248]. Beltowska-Lehman, E., Indyka, P., Bigos, A., Szczerba, M. J., Guspiel, J., Koscielny, H., Kot, M. (2016). Effect of current density on properties of Ni–W nanocomposite coatings reinforced with zirconia particles. *Materials Chemistry and Physics*, 173, 524–533. doi:10.1016/j.matchemphys.2016.02.050.

- [249]. Xia, X., Zhitomirsky, I., McDermid, J. R. (2009). Electrodeposition of zinc and composite zinc–yttria stabilized zirconia coatings. *Journal of Materials Processing Technology*, 209(5), 2632–2640. doi:10.1016/j.jmatprotec.2008.06.031.
- [250]. Zheng, H.-Y., An, Mao-Zhong (2008). Electrodeposition of Zn–Ni–Al₂O₃ nanocomposite coatings under ultrasound conditions. *Journal of Alloys and Compounds*, 459(1-2), 548–552. doi:10.1016/j.jallcom.2007.05.043.
- [252]. Abdel-Karim, R., Reda, Y., Muhammed, M., El-Raghy, S., Shoeib, M., Ahmed, H. (2011). Electrodeposition and Characterization of Nanocrystalline Ni-Fe Alloys. *Journal of Nanomaterials*, 2011, 1–8. doi:10.1155/2011/519274.
- [253]. Abdallah, B., Jazmati, A. K., Refaai, R. (2017). Oxygen Effect on Structural and Optical Properties of ZnO Thin Films Deposited by RF Magnetron Sputtering. *Materials Research*, 20(3), 607–612. doi:10.1590/1980-5373-mr-2016-0478
- [254]. Matsumiya, M. (2015). Nucleation Behaviors of Nd and Dy in TFSA-Based Ionic Liquids. Electroplating of Nanostructures. doi:10.5772/61292.
- [286]. ASTM E–384-05a, Standard Test Method for Microindentation Hardness of Materials. <https://www.koopaco.com/Content/file/ASTM-E384.pdf>.
- [280]. Paterlini, T. T., Nogueira, L. F. B., Tovani, C. B., Cruz, M. A. E., Derradi, R., Ramos, A. P. (2017). The role played by modified bioinspired surfaces in interfacial properties of biomaterials. *Biophysical Reviews*, 9(5), 683–698. doi:10.1007/s12551-017-0306-2.
- [287]. G. Cârâc, C. Iticescu, L. Benea, T. Lampke, S. Steinhauser (2007). The effect of nano-Al₂O₃ dispersed phase in nickel matrix electrocodeposited. *Revue Roumaine de Chimie* 52(11), 1057–1062. http://revroum.lew.ro/wp-content/uploads/2007/RRCh_11_2007/Art%2007.pdf
- [288]. Wenzel, R. N. (1936). Resistance of solid surfaces to wetting by water. *Industrial & Engineering Chemistry*, 28(8), 988–994. doi:10.1021/ie50320a024.
- [289]. Wolansky, G., Marmur, A. (1999). Apparent contact angles on rough surfaces: the Wenzel equation revisited. *Colloids and Surfaces A: Physicochemical and Engineering Aspects*, 156(1-3), 381–388. doi:10.1016/s0927-7757(99)00098-9
- [290]. Berradja, A., Bratu, F., Benea, L., Willems, G., Celis, J.-P. (2006). Effect of sliding wear on tribocorrosion behaviour of stainless steels in a Ringer’s solution. *Wear*, 261(9), 987–993. <https://doi.org/10.1016/j.wear.2006.03.003>
- [298]. Zhang, H. (2016). Surface characterization techniques for polyurethane biomaterials. *Advances in Polyurethane Biomaterials*, 23–73. doi:10.1016/b978-0-08-100614-6.00002-0
- [301]. Sun, X., Yang, G., Song, W., Li, J., Ma, Y., Zhou, Y. (2012). Wear performance of Ni/ZrO₂ infiltrated composite layer. *Journal of Wuhan University of Technology-Mater. Sci. Ed.*, 27(1), 73–78. doi:10.1007/s11595-012-0410-x.
- [302]. Xue, Y.-J., Jia, X.-Z., Zhou, Y.-W., Ma, W., Li, J.-S. (2006). Tribological performance of Ni–CeO₂ composite coatings by electrodeposition. *Surface and Coatings Technology*, 200 (20-21), 5677–5681. doi:10.1016/j.surfcoat.2005.08.002.

-- // --

